Unclassified
SECURITY CLASSIFICATION OF THIS PAGE

REPORT DOCUMENTATION PAGE

Form Approved
OMB No. 0704-0188

1a. REPORT SECURITY CLASSIFICATION Unclassified	1b. RESTRICTIVE MARKINGS
2a. SECURITY CLASSIFICATION AUTHORITY	3. DISTRIBUTION / AVAILABILITY OF REPORT Approved for public release; Distribution is unlimited.
2b. DECLASSIFICATION / DOWNGRADING SCHEDULE	
4. PERFORMING ORGANIZATION REPORT NUMBER(S)	5. MONITORING ORGANIZATION REPORT NUMBER(S)
6a. NAME OF PERFORMING ORGANIZATION Georgia Institute of Tech. School of Aerospace Eng. — 6b. OFFICE SYMBOL (*If applicable*)	7a. NAME OF MONITORING ORGANIZATION Office of Naval Research
6c. ADDRESS (*City, State, and ZIP Code*)	7b. ADDRESS (*City, State, and ZIP Code*)
8a. NAME OF FUNDING / SPONSORING ORGANIZATION — 8b. OFFICE SYMBOL (*If applicable*)	9. PROCUREMENT INSTRUMENT IDENTIFICATION NUMBER N00014-93-1-1349
8c. ADDRESS (*City, State, and ZIP Code*)	10. SOURCE OF FUNDING NUMBERS PROGRAM ELEMENT NO. — PROJECT NO. — TASK NO. — WORK UNIT ACCESSION NO.

DTIC ELECTED OCT 10 1995 G

11. TITLE (*Include Security Classification*)
Controlling Mechanisms of Pulsating Incineration Processes

12. PERSONAL AUTHOR(S)
B.T.Zinn, J.I.Jagoda, L.M.Matta

13a. TYPE OF REPORT	13b. TIME COVERED	14. DATE OF REPORT (*Year, Month, Day*)	15. PAGE COUNT
Annual Technical	FROM 10/1/94 TO 9/30/95	9/30/95	45

16. SUPPLEMENTARY NOTATION

17. COSATI CODES			18. SUBJECT TERMS (*Continue on reverse if necessary and identify by block number*)
FIELD	GROUP	SUB-GROUP	Pulsed Combustion, Incineration, Jet Excitation, Sublimation, Bifurcating jet

19. ABSTRACT (*Continue on reverse if necessary and identify by block number*)

SEE BACK

19951006 054

20. DISTRIBUTION / AVAILABILITY OF ABSTRACT	21. ABSTRACT SECURITY CLASSIFICATION
☒ UNCLASSIFIED/UNLIMITED ☒ SAME AS RPT. ☐ DTIC USERS	Unclassified
22a. NAME OF RESPONSIBLE INDIVIDUAL	22b. TELEPHONE (*include Area Code*) — 22c. OFFICE SYMBOL

Annual Technical Report

CONTROLLING MECHANISMS OF PULSATING INCINERATION PROCESSES

ONR Grant No. N00014-93-1-1349

September 30, 1995

Prepared For:

Office of Naval Research

Accesion For

NTIS CRA&I ☒
DTIC TAB ☐
Unannounced ☐
Justification .....

By .....
Distribution /

Availability Codes

Dist	Avail and / or Special
A-1	

Contract Monitors:

Dr. Klaus Shadow

and

Dr. Judah Goldwasser

Prepared By:

B. T. Zinn

J. I. Jagoda

L. M. Matta

School of Aerospace Engineering

Georgia Institute of Technology

Atlanta, GA 30332

Approved for public release;

Distribution is unlimited.

Abstract

The purpose of this research program is to study the fundamental processes that control the performance of acoustically excited incineration systems. The information learned will be used in the development of a compact, high-efficiency waste incinerator for shipboard use. Tests performed during the current reporting period of this program have demonstrated that mixing and heat transport processes, both crucial to the incineration process, may be enhanced by imposing acoustic pressure oscillations. Because the combustion efficiency and pollutant emission characteristics of incinerators are directly affected by the mixing of in-flowing air with fuel, acoustic control of turbulent jets is of interest to the development of compact incinerators. Studies of jets subjected to transverse mode oscillations have shown that, under the proper conditions, the jet will shed large, alternating, vortical structures that can cause the jet to bifurcate. This process results in a greater spatial mixing rate. Transverse mode acoustic forcing had the greatest effect in the range of St = 0.2 - 0.3. The effect of acoustic oscillations upon solid fuel pyrolysis was investigated by studying the effect of acoustic oscillations upon dry ice sublimation. This study showed that the presence of pulsations enhanced the sublimation process, which strongly suggests that they would also enhance the processes involved in incinerating solid wastes. Also, a model incinerator that can burn liquid and solid waste surrogates in the presence of transverse and multi-dimensional mode acoustic oscillations has been developed. This facility will be used to measure the effects of acoustic oscillations on burning rate, soot production and burnout, and NOx, CO, CO_2 and UHC levels present in the exhaust.

Introduction

The goal of waste incineration is to completely burn the combustible portion of the waste material without emitting hazardous substances into the environment. The incineration of solid wastes generally proceeds through a number of individual processes, which, depending upon the phase of the waste, may include heating of the waste, evaporation of its water content, devolatilization, pyrolysis, mixing of gaseous fuel and oxidizer, ignition, and combustion. In order to obtain complete incineration within the limited volume of a compact incinerator, the rates of all the above listed processes must be high. At present, high gas phase mixing rates are generally attained by providing the incinerator with an air flow rate that is considerably higher than that required for a stoichiometric combustion process. This reduces the global fuel/air ratio within the incinerator, resulting in lower reaction temperatures. Thus, while high air flow rates promote faster gas phase mixing and increase the rate of convective heat transfer between the gas phase and the solid waste, the effect is compensated by lower temperatures and the resulting reduction in waste heating rates and slower chemical kinetics.

The identification of processes and the development of techniques that can enhance the rates of various transport processes are crucial to the development of incinerators that are more compact, more efficient and emit less pollutants than state of the art incineration systems. Recent investigations have demonstrated that the presence of acoustic oscillations and flow pulsations can increase the rates of transport processes. Patera et. al.,[1,2] for example, have shown that mixing and heat transfer rates in laminar flow in a channel can be considerably increased by oscillating the flow rate into the channel at a frequency at which the flow's shear layer is unstable. While there is considerable evidence that mass[3] and heat[4,5,6] transfer rates are increased by acoustic oscillations, the precise mechanisms responsible for these increases are not entirely understood. Strong evidence[4,7] suggests that the increased transport rates are due to the excitation of turbulence and vortical structures by the acoustic oscillations. In a study by Vermeulen et al.,[8] flow oscillations were shown to reduce flow stratification and improve mixing. This was demonstrated by the elimination of localized pockets of high temperature gas, or "hot spots", at the exit plane of a gas turbine combustor, which can damage turbine blades downstream of the combustor. The capability to reduce or eliminate this type of local stratification is of practical importance in incinerators because non-uniform loading of waste materials leads to fuel rich regions in the incinerator, which can result in the emission of "puffs" consisting of soot, CO, and unburned hydrocarbons. Also, "hot spots" may be the cause of increased thermal nitrogen oxide production by the Zeldovich mechanism.

Results of several investigations of pulse combustors suggest that when combustion occurs in an oscillatory flow field, the combustion time is reduced and combustion efficiencies are increased with respect to combustion in a steady flow field. For example, Lyman[9] showed that

pulsations increased the burning rates of individual coal particles, and Zinn et al.[10] found that unpulverized coal nuggets can be burned in a Rijke type pulse combustor with high combustion efficiency while utilizing little excess air. Bai et al.[11] showed that heavy fuel oils, which are generally difficult to burn, can be burned with high combustion efficiencies in a pulse combustor specifically designed for this purpose.

A recent study supported by the EPA investigated the effects of pulsations upon the incineration process.[12] In the study, a tunable pulse combustor was retrofitted to an existing EPA rotary kiln incinerator simulator and used to excite large amplitude acoustic oscillations within the incinerator. Toluene and polyethylene were burned as surrogates for hazardous and municipal wastes, respectively. Pulsations were shown to reduce the magnitude of "puffs" and soot emissions. Interestingly, reductions in soot emissions observed when burning toluene with pulsations were, in some cases, accompanied by increased levels of CO and hydrocarbon emissions. In contrast, when polyethylene was burned in the presence of pulsations, the emissions of soot, CO, and hydrocarbons were all reduced. In both cases, the pulsations reduced the O_2 concentrations in the exhaust to very low levels, indicating that the pulsations improved the utilization of available oxygen in the incineration process.

Research Accomplishments

The objective of the present study is to investigate the mechanisms through which pulsations affect the incineration process in order to obtain information that will aid the development of an efficient and compact incinerator for ship-board use. Specifically, the effects of acoustics on the mixing rates, flow characteristics, burning rates of solid and liquid wastes, and soot, NO_X, CO, and unburned hydrocarbon emissions are being investigated in simulated incinerators.

Transverse Excitation of a Jet:

The main objective of acoustic excitation of free jets is to gain control of the processes that govern the downstream evolution of the jet, generally with the goal of increasing the rate of mixing of the jet with the surrounding flow. Because the burning efficiency and pollutant emission characteristics of combustion processes are directly affected by the mixing of the reactants, acoustic control of turbulent jets is of interest to the development of compact waste incinerators.

The effects of acoustic and mechanical excitation on shear layers and jets has long been the subject of investigation. An overview of the available information on this subject can be found in reviews by Cantwell[13] and Ho and Huerre[14]. It has been shown that the formation and pairing of large, coherent vortices in jet flows can be affected by excitation (for example, Refs. 15-20). By

modifying the size and character of the large scale structures, the spreading rate and entrainment of the jet can be influenced.

Transverse and three-dimensional mode oscillations are of interest because of the potential application to combustor cavities in which such modes are often more easily excited than purely longitudinal modes. Ogawa et al.[21] showed that, by using speakers perpendicular to the axis of a jet to provide excitation, the time-averaged cross section of the jet could be distorted to have an elliptical shape. The goals of the present study were to determine whether such a phenomenon would be observed in a ducted jet, to investigate the role of large scale, coherent vortices in the elliptical jet, and to study the effect of this behavior on entrainment and mixing. Under the current program, the affects of transverse mode, standing, acoustic oscillations on the characteristics of a turbulent, circular jet of air were investigated in two different experimental configurations.

In the first experimental configuration, transverse, resonant oscillations were used to excite a subsonic, axisymmetric jet discharging into a rectangular enclosure with inside dimensions of 20.3cm (8in.) wide x 12.7cm (5in.) high x 68.6cm (27in.) long. The configuration of this facility is shown schematically in Fig. 1. The top, the downstream end, and one side of the facility are constructed of acrylic to enable visualization of the jet from various angles. The dimensions of the cavity were chosen so that resonant acoustic modes would not occur at redundant frequencies. The jet was introduced into the duct through a 61cm (24in.) long, 1.1cm ID (0.43in.) stainless steel tube. A stream of tobacco smoke was injected at low velocity through a 2.5mm (0.1in.) annulus around the jet exit to make the shear layer visible.

Transverse mode, standing, acoustic oscillations were excited in the duct using two 100W, Atlas, compression-type, siren drivers mounted on opposing walls near the downstream end of the duct, as shown in Fig. 1. While the position of the drivers near the downstream end of the duct reduces their efficiency in forcing purely transverse mode oscillations, it was necessary to place them as far as possible downstream of the jet inlet to minimize the effects of mean flow disturbances which arise in the vicinity of the acoustic drivers[22]. Acoustic pressures were measured using Kistler piezoelectric pressure transducers.

A light sheet, which was approximately 1.9mm (0.075in.) thick at the investigated region, formed from the beam of a Metalaser Technologies 20W copper vapor laser by a combination of spherical and cylindrical lenses was used to illuminate a planer slice of the jet for visualization. The pulse rate of the laser can be adjusted from 2 to 10kHz, and the pulse width is nominally 30ns FWHM. The short pulse width of the Cu vapor laser is excellently suited to stop-motion photography in high speed flows. Because the lenses used were not achromatic, the yellow light at 578nm and the green light at 511nm had beam waists at different locations. To correct for this, the yellow light was deflected from the beam with a mirror that reflects light at 578nm and transmits light at 511nm. Only the green light was used for visualization. The laser sheet was

directed along the axis of the jet, and could be oriented either in or perpendicular to the plane of the transverse mode, standing, acoustic oscillation.

Images of the flow in the illuminated plane were recorded using a Kodak EktaPro intensified motion analyzer. This CCD based system allows a maximum full-frame collection rate of 1000 frames/sec, and up to 12,000 frames/sec by reducing the frame size. The camera provides 8 bit gray scale response and has a full-frame resolution of 239 x 192 pixels.. The imaging system is equipped with enough memory to store 3600 full size frames, which can then be downloaded to a PC for analysis and storage using an IEEE 488 interface. The camera was synchronized with the pulses of the laser to assure that each image resulted from a single laser pulse.

Visualization of the coaxial jet indicates the presence of three distinct regions in the flow: 1) unmixed smoke in the shear layer that scatters much of the incident laser light is indicated by bright regions, 2) the core region of the jet where no smoke has penetrated appears dark, and 3) regions where the smoke and air are mixed are indicated by regions of medium intensity in the images. Figure 2a shows a side view of the jet without oscillations. When oscillations were excited, the jet was observed to 'flap' back and forth in the plane of the oscillations as large scale coherent vortical structures were alternately shed from opposite sides of the jet inlet, as shown in Fig. 2b. No visible vortex shedding was observed in the plane perpendicular to the oscillations. This behavior causes the excited jet to have, in a time-averaged sense, an elliptical cross section.

In all the following tests, the forcing occurred at a frequency of 855Hz, which corresponds to the fundamental mode in the 20.3cm dimension of the cavity. In this mode, the jet entered the cavity at a position where the acoustic velocity (which is perpendicular to the direction of the jet) is maximum. By dividing the jet exit velocity by the measured distance between vortices it was determined that each side of the jet sheds one vortex per acoustic cycle, and that the opposing vortices are shed 180° out of phase. These structures are then convicted downstream by the mean flow.

Figure 3 shows a sequence of images in which the jet exit velocity is 31m/s (101.4ft/s) and the amplitude of the oscillation was varied from no sound to 948Pa RMS (154dB). A pressure amplitude of 948Pa RMS corresponds to a velocity amplitude of approximately 3.3m/s 0 to peak. The phase of oscillation at which these images were obtained was not fixed, therefore the stage of vortex shedding in each image varies. It is observed that the size of the vortex structures shed from the jet mouth depends upon the amplitude of the oscillation.

Time averaged images in which the jet exit velocity is 31m/s (101.4ft/s) for various amplitudes of oscillation are shown in Fig. 4. These images were used to measure the effect of the sound amplitude on the effective spreading angle of the jet and on the jet core length, which provide measures of the scale of the induced vortical structures. The data in Fig. 5 show that as the amplitude increases, the length of the jet core decreases. The rate of shortening decreases as

the amplitude increases, which is to be expected, since the core length can never reach zero. The angle of the outer edge of the mixing layer is also graphed in the figure as a function of the oscillation amplitude.

The frames shown in Fig. 6 show four tests in which the jet velocity was varied and the amplitude of the acoustic oscillation was held fixed at 632Pa RMS (150 dB). The jet velocity ranged from 10.3m/s (33.8ft/s) to 41.2m/s (135.2ft/s). The frequency was held fixed at 855Hz, resulting in a variation of Strouhal number from 0.91 to 0.23. The images suggest that, over the investigated range, the size of the structures shed from the jet exit plane increase with the jet velocity, while the time over which these structures are coherent decreases. The vortex structures observed in the image of the 10.3m/s jet are small, distinctly formed and remain coherent for approximately three convective wavelengths (3.3 jet diameters). At a jet velocity of 41.2m/s, the alternating nature of the vortex shedding causes the jet to flap back and forth. The structures of the vortices are less clear at this velocity, and the vortices appear to lose coherency after about 1 convective wavelength (4.4 jet diameters). While the length over which these structures remains coherent increases with the jet exit velocity, the time of coherence decreases from approximately 3.5ms at 10.3m/s to about 1.2ms at 41.2m/s.

Time averaged images for tests in which the jet velocity was varied and the amplitude of the acoustic oscillation was held fixed at 632Pa RMS (150 dB) are shown in Fig. 7. From these images, the effect of the Strouhal number on the effective spreading angle of the jet and on the jet core length can be determined. Figure. 8 shows the half angle of the outer edge of the jet in the plane of the acoustic oscillation as a function of the Strouhal number. For comparison, data showing the effect of the Strouhal number on the spread angle of the jet with no oscillations present is also shown, and as expected, is independent of the jet velocity. On the other hand, experiments with transverse acoustic oscillations present in the cavity show that the spread angle of the jet in the plane of the oscillations has a maximum of about 60 degrees that occurs near St = 0.5. Figure 9, which shows the measured jet core lengths versus Strouhal number with and without oscillations, shows similar results. The jet core length is shown to have a minimum value of about 1.3 jet diameters near St = 0.5. The jet core length is shown to be independent of the jet velocity when no oscillations are present.

While the experimental facility shown in Fig. 1 offers a fairly good model of air flow into an incinerator, the recirculation of the mixed smoke and air causes difficulty in measurement of the mixing rate and results in generally poor conditions for visualization of the vortical processes involved. Therefore, a second facility was developed to minimize recirculation and provide better conditions for studying the effect of resonant, transverse, acoustic oscillations on the mixing of a jet with the surrounding fluid. In this facility, a subsonic, axisymmetric jet discharged into a duct with a 12 in. (30.5 cm) square cross-section that was open upstream and downstream of the jet.

The facility is shown schematically in Fig. 10. In this configuration, the jet induces a mean flow of air through the duct by entrainment. In this configuration, standing acoustic oscillations can be excited transverse to the jet flow while avoiding the recirculation patterns associated with a rapid area change (i.e., a dump plane). For visualization and optical measurements, the air jet was seeded with cooled tobacco smoke using a developed "cigarette smoking system". The jet was introduced into the duct through a 36in. (91.4cm) long, 0.425in. (1.08cm) ID stainless steel tube. Transverse mode, standing, acoustic oscillations were excited in the duct using two, 100W, Atlas, compression-type siren drivers mounted on two opposing walls near the downstream end of the duct. Dynamic pressures were measured using Kistler piezoelectric pressure transducers, and mean velocities were measured using a Pitot probe and a Datametrics Barocel pressure sensor.

The resonant mode excited in the duct was chosen so that exit plane of the jet would be subjected to the greatest possible transverse velocity oscillation. The excited acoustic field in the duct was characterized by mapping the pressure distribution in cross-sections perpendicular to the flow axis. Pressure amplitudes were measured on an 81 point grid transverse to the jet at four axial locations in the duct. The measured pressure distributions, shown in Fig. 11, were similar at each of the four axial locations. Lighter regions in the plots show regions of highest pressure oscillation. The measured distribution is slightly tilted, which is believed to be due to misalignment of the drivers.

Measurements of the mean velocity with and without oscillations present were performed along the horizontal and vertical axes of the duct using a Pitot probe inserted from the downstream end of the duct. Each average velocity was calculated from 500 samples collected at 100Hz. Due to the nature of the measurement, the relative error increases as the measured velocity decreases. Therefore, the accuracy of measurements below about 2m/s (6.6ft/s) are highly suspect.

Comparisons of the velocity profiles in the vertical axis (in the direction of the acoustic oscillations) are shown in Fig. 12. At each of the three axial locations measured, the presence of oscillations resulted in a wider velocity profile. Even more interesting. however, is the fact that the profile at 13.65cm (5.4in.) downstream of the jet exit plane is obviously bimodal. This suggests that either the jet was flapping in the direction of the oscillations, or that the velocity oscillation caused the jet to bifurcate. Such jet bifurcation phenomena was observed by Reynolds et. al. in several studies on jet excitation[19,20,23], but from these studies it was concluded that a combination of axial and transverse excitation was required to bifurcate the jet. Comparisons between the unexcited and excited mean velocity profiles perpendicular to the direction of the oscillations are shown in Fig. 13. No broadening of the jet is evident in this direction.

Flow visualization was used to determine whether the broadening of the velocity profile was due to flapping or bifurcation of the jet. For this purpose, smoke was seeded into the jet, and Mie

scattering of a laser sheet produced from a Coherent Innova 70, 5W Argon-ion laser was observed. The sheet could be introduced into the duct either from the downstream end, which allowed a planer slice of the jet to be observed, or through the side of the duct, which provided cross-sectional views of the jet at various downstream locations. At a shutter speed of 10μs, even at the highest mean centerline velocity of 52m/s, a particle of smoke would have only traveled 0.52mm (0.02in.) during the exposure. Also, at the excited frequency of 585 Hz, 10μs corresponds to approximately 0.6% of one acoustic period. Therefore, images were considered to be instantaneous. In order to decouple the periodic phenomena from turbulent processes, the camera was triggered at a constant phase of the acoustic cycle and images were time averaged over a number of these phase-locked frames. All cross-sectional images shown in this report were taken at 13.65cm downstream.

Figure 14 shows phase-locked, averaged images of the jet with and without oscillations present. The laser sheet lies in the plane of the oscillations, and the broadening of the jet due to the presence of the oscillations is evident. The frequency of the oscillation is 585Hz., and the amplitude is 134dB. The mean velocity at the jet exit is 24.4m/s (80ft/s), which corresponds to a Reynolds number based on diameter of approximately 18000. Near the mouth of the jet, the smoke follows a sinuous pattern, caused by alternating vortex shedding from the jet exit. These vortices lose coherence about two convective wavelengths downstream from the jet.

The unexcited, instantaneous images show roughly circular distributions with dark, high concentration cores and light, low concentration fringes. A typical image is shown in Fig. 15a. Light and dark pockets at the fringe and core are distributed randomly. The excited, instantaneous images, of which a typical image is shown in Fig. 15b, show highly distorted distributions, in which the core is stretched in line with the excitation direction, apparently bifurcating in some instances. The angle of the tilt is consistent with the results seen in the pressure field measurements, where the symmetry of the line of excitation was shown to be slightly off the vertical centerline.

Comparing the averaged images of the unexcited and excited jet in Fig. 16 shows a distinct effect due to the acoustics. The spreading of the jet in the direction of the excitation is clearly due to bifurcation, because there are two visible jet cores at the same instant. This is consistent with the results seen in the velocity profiles.

In order to quantify the effect of the bifurcation on the spatial mixing rate, a computer code was developed that used pixel intensities to compute a quantity that represents the entropy of mixing from instantaneous cross-sectional images. This procedure was based on a similar technique by Everson et. al.[24] The state at the exit of the jet, where virtually no mixing has taken place between the jet and the surrounding air, is considered to have zero entropy. The state far downstream, where the smoke and the entrained air are uniformly distributed, was considered to

be the maximum entropy state, and was used to normalize the measured entropy values. Since the analysis of each frame used the total intensity as a normalization factor, variations in the total intensity from image to image were made inconsequential. Results could be compared between runs even if the smoke seeding rate, laser brightness, or gain of the camera varied, as long as the camera did not overrange. Due to the turbulent nature of the mixing process, the entropy varies over time. Therefore, the entropies were calculated for 100 instantaneous frames and then averaged. Note that this produces quite a different result from calculating the entropy of an averaged image.

Figure 17 shows a plot of the change in entropy with the jet exit velocity. The entropy of mixing for the acoustically excited jet is consistently higher than that of the unexcited jet. The plot of the change in entropy between the excited and unexcited jets shown in Fig. 18 suggests a peak effect when the Strouhal number is between 0.2 and 0.3. This does not correspond exactly to the results of the previous experiment, where the maximum spreading angle was observed to occur at a Strouhal number of 0.5. This may be due to the presence of the recirculation region in the first experiment, which could affect the vortex shedding process. It is also true that, in studies of acoustically excited jets, the preferred Strouhal numbers are not constant. The peak Strouhal number reported by Vlasov and Ginevskii[25] is 0.5, Crow and Champagne[26] report 0.3, and Lepicovsky[27] et. al suggest a range between 0.4 and 0.5. Therefore, it may be concluded that the present for transverse mode excitation are not completely inconsistent with previous jet excitation studies. It is also possible that the spreading angle of the jet measured in the first facility does not correctly represent the mixing rate.

The data plotted in Fig. 19 show the effect of the amplitude of oscillation on the entropy of mixing. The three curves shown represent different jet exit velocities, and therefore, different Strouhal numbers. While the possible error at the lowest sound pressure level is estimated to be 5%, the curves all show increased mixing with increased amplitude. It is also clear that while the jets with velocities of 22.13m/s (72.6ft/s) and 25.22m/s (82.75ft/s), which correspond to Strouhal numbers of 0.29 and 0.25, respectively, are affected very similarly by the amplitude of the oscillation, the jet at 12.35m/s (40.5ft/s), St = 0.52, is much less sensitive to the amplitude. Note that the curves appear roughly linear with amplitude in decibels, which suggests an exponential dependence of the mixing rate upon the pressure.

Sublimation Rate and Heat Transfer Studies:

Testing is currently underway to determine the effect of the acoustic oscillations on the sublimation rate of dry ice (solid carbon dioxide) in the simulated incinerator. Dry ice was chosen as a waste surrogate for cold flow testing for two reasons. First, the sublimation of dry ice is a good model for the pyrolysis of solid fuels, because the rate of sublimation depends upon the heat

transfer rate and mass is transferred away in gas phase. Second, due to the presence of a small amount of water (generally less than 1%) trapped in the dry ice during the manufacturing process, it produces a visible "fog" as it sublimes.

Figure 20 provides schematic diagrams of the setup for this experiment. The facility consists of a rectangular wood and acrylic box with an air inlet on one end and exhaust port on the opposite end. The acoustic amplitude is determined using pressure transducers mounted on the walls. Speakers are mounted to opposing walls near the downstream end of the cavity. The dry ice block is positioned at 1/4 of the axial length of the box and centered between the sides. Dry ice for this experiment was produced using an Insta-Ice, 454g (1lb.) capacity, dry ice form and standard 22.7kg (50lbs.) cylinders of commercial grade CO_2.

The images in Fig. 21 show the fog layer at the downstream corner of the dry ice block. The top left picture shows the thin, uniform layer present in the absence of mean flow and acoustic oscillations. The picture on the top right shows the same block subjected to the maximum velocity of a 150dB oscillation that is directed left and right across the page. A vortical structure is produced at the corner of the block. In the image at the bottom left, a mean flow of air is being injected into the chamber (from left to right) at 0.5m/s (1.6ft/s) without acoustics. Small structures are present in the boundary layer that are convected downstream by the flow. And finally, in the image at the bottom right, the same mean flow is present and a 150dB oscillation is excited. In this case, the addition of the convective flow and the acoustically generated structure appears more chaotic than the purely acoustic phenomenon.

Preliminary testing and flow visualization suggested that the imposed oscillations have the greatest effect when the ice block was positioned at a velocity maximum. Therefore, for the series of tests reported here, oscillations were excited at the fundamental transverse mode of the cavity. Because the temperature of the gas in the cavity was dependent upon the heat transfer to the ice block, the resonant frequency (which was on the order of 800Hz) varied slowly with time. To compensate for this, the driving frequency and amplitude were periodically corrected. The amplitude of the oscillation was never allowed to vary more than 5% during a run.

The outgoing flow from the chamber was sampled with a Beckman model 864 infrared CO_2 analyzer to measure the percentage of carbon dioxide present. These values were then recorded over a 45 minute run time using the LabVIEW data acquisition computer program and an IOTech 488/8SA A/D converter. From these data and the known flow rate of incoming air, the amount of excess CO_2 sublimated from the block of dry ice was calculated. A second, much simpler but less accurate technique was used to provide a check of the exhaust gas measurements. A digital balance was used to measure the mass of the dry ice block at the start and conclusion of each 45 minute test. Since the difference of these masses should equal the mass of CO_2 lost by the dry ice

block, this value was compared to the amount calculated from the exhaust gas analysis technique described above.

The maximum pressure oscillation that can be forced at the chosen resonant mode is about 157dB. The corresponding velocity oscillation at test conditions is approximately 2.5m/s (8.2ft/s). Therefore, the mean flow velocity of air into the chamber was set to 1.0m/s (3.3ft/s) for the reported tests. This allowed testing with acoustic velocities that were both above and below the mean flow velocity.

A time sequence of events was established to maintain as much repeatability of conditions between runs as possible. This sequence included making a dry ice block, weighing the block, placing the block in the facility, triggering the data acquisition system, and initiating the acoustic driving. In order to establish the repeatability of the procedure, a series of tests was performed in which the start-up procedure was followed but no acoustic driving was used. The results of this series of tests is shown in Fig. 22. The curves show that it takes about 1min for the cavity to reach operating conditions and for the exhaust gas to pass through the sampling system. After this period has passed, the repeatability is about 0.3L/m (0.01cf/m).

Series of experiments were performed at six amplitudes of acoustic excitation, ranging from no excitation to 155dB. The data in Fig. 23 show the results from a typical test. The acoustic driving is initiated at 2min into the run, which accounts for the discontinuity apparent in some of the curves at that time. A comparison of the measured change in mass of the dry ice block during a run to the sublimated mass calculated from the sampled exhaust gas is shown in Fig. 24. It is not clear at this time why the calculated change in mass is consistently 30% higher than the measured change, but the trends are the same.

It is clear from the data that the sublimation rate increases in the presence of acoustic excitation. The significance of the increase depends upon the amplitude of the oscillations. Under the test conditions, it appears that an amplitude of 150dB is needed before the effects of the oscillations become evident, and an amplitude at or above 155dB is necessary before these effects become significant. It is interesting to note that it is between 145dB and 150dB (the exact amplitude depends on the gas temperature in the chamber) that the acoustic velocity becomes greater than the mean injection velocity. This fact could be very important, and further testing is needed at different mean flow velocities in order to determine whether the acoustic velocity must be greater than the mean flow velocity for oscillations to significantly affect the sublimation rate or if this is a purely coincidental result of the chosen test conditions. Future test plans also include driving at higher amplitudes to see if the trend continues.

Pulsed Incineration Facility:

For the combustion phase of this study, a model incinerator capable of burning liquid and solid waste surrogates in the presence of transverse and multi-dimensional mode acoustic oscillations has been developed. This facility will be used to measure the effects of acoustic oscillations on soot production and burnout as well as NOx, CO, CO_2 and UHC levels present in the incinerator exhaust. If time permits, acetone, O_2 and OH PLIF may be used to visualize the differences in the flame structure with and without oscillations.

A schematic of the facility is shown in Fig. 25. The majority of the combustor is made of carbon steel, with the exceptions of an access panel in the top, which is aluminum, and the fused quartz windows. The bottom surface of the combustor is fitted with blow-out panels that are designed to pop off before the windows shatter in the event of an explosion. The side panels are constructed to be modular, so that the windows, the acoustic drivers, and all wall-mounted instrumentation can be repositioned wherever desired. The aluminum, liquid fuel burner is 5cm (2in.) square and 1.9cm (3/4in.) high. The acoustic drivers are 100W Atlas siren drivers, and air cooling is provided to prevent burning of the diaphragms. The amplitude of the pressure oscillation is measured with a water cooled, Kistler piezoelectric pressure transducer, and a second transducer mounted to a probe allows for characterization of the pressure away from the wall. Temperatures are measured using an array of Omega thermocouples inside the combustor and an additional thermocouple in the exhaust section.

The acoustic driving in the incinerator is achieved through either open or closed loop operation. In open loop operation, a signal to the drivers is provided by a function generator at a chosen frequency. In closed loop active control operation, the acoustic pressure signal in the chamber, measured using a piezoelectric pressure transducer, is amplified, phase-shifted, and fed back into the acoustic drivers. By adjusting the gain, phase-shift, and the position of the pressure probe, the system can be tuned to resonate in various acoustic modes. While open loop operation is advantageous in its simplicity and constant frequency, closed loop active control provides the benefit of finding and 'locking on' to various resonant modes. This benefit is quite useful in the incinerator, because acoustic driving affects the temperature distribution in the combustion chamber, which causes the resonant frequency to be somewhat dependent on the amplitude of the oscillation..

Liquid fuel is fed into the burner using a system described in Fig. 26. The pump supplies fuel to both the burner and the leveling vessel at a rate faster than it is being burned. Excess fuel overflows into the standpipe flows back to the pump reservoir. The leveling vessel is mounted to a micrometer that controls its height, and therefore, the fuel level in the burner. The burning rate is determined by measuring the rate of decrease of fuel in the reservoir. The flame is extinguished by dumping the fuel from the burner by opening the control valve.

Currently, the facility is being used to measure the effects of acoustic oscillations on the burning rate of the fuel and the amount of NOx, CO, CO_2, O_2 and UHC present in the incinerator exhaust. These tests are planned for a variety of liquid fuels, including methanol, methanol/gasoline mixtures, and methanol/toluene mixtures, and for solid fuels including polyethylene and toluene impregnated cotton. In addition, soot generation and burnout will be measured using the laser extinction technique in both the combustor and the exhaust. Additionally, if time permits, preparations are underway to seed the fuel with acetone so that a combination of acetone, O_2 and OH PLIF may be used to visualize the differences in the flame structure with and without oscillations. A tunable KrF excimer laser and an excimer pumped dye laser are available for PLIF measurements.

Summary and Conclusions

The objective of the present study is to investigate the mechanisms through which pulsations affect the incineration process in order to obtain information that will aid the development of an efficient and compact incinerator for ship-board use. Specifically, the effects of acoustics on the mixing rates, flow characteristics, burning rates of solid and liquid wastes, and soot, NO_X, CO, CO_2 and unburned hydrocarbon emissions are being investigated in facilities designed to simulate a compact incinerator.

In this reporting period, the effects of transverse acoustic excitation on a jet were investigated. In one configuration, transverse, resonant oscillations were used to excite a subsonic, axisymmetric jet discharging into a rectangular enclosure. It was observed that this forcing caused the jet to flap in the plane of the oscillations. This flapping motion resulted from the shedding of vortices from alternating edges of the jet mouth, which were subsequently convected downstream. The vortex generation was confined to the plane of the oscillation, which caused the jet to have an elliptical cross section on average. In time averaged images, it was observed that the spreading rate of the jet could be significantly enhanced by the presence of transverse acoustic oscillations.

Continuation of this study in a facility designed to avoid the recirculation region typical of a dump plane added further insight into the jet spreading phenomenon. Mean velocity measurements and flow visualization studies revealed that, while flapping of the jet occurs near the exit of the jet, bifurcation of the jet can occur further downstream. A developed technique to measure the entropy of mixing from a cross-sectional image of the jet was used to quantify the increased spatial mixing rate of the bifurcated jet. It was determined that transverse acoustic forcing had the greatest effect on mixing over a Strouhal number range of 0.2 to 0.3.

Tests were performed to determine the effect of acoustic oscillations on the sublimation rate of dry ice in the simulated incinerator. Results show that the sublimation rate increases in the presence of acoustic excitation. The data shows that the effects of the acoustics become significant at amplitudes above 150dB. Further testing is needed to determine the nature of this threshold.

Finally, a model incinerator capable of burning a variety of liquid and solid waste surrogates in the presence of transverse and multi-dimensional mode acoustic oscillations has been developed. This facility will be used to measure the effects of acoustic oscillations on burning rate, soot production and burnout, and NOx, CO, CO_2 and UHC levels present in the incinerator exhaust. If time permits, acetone, O_2 and OH PLIF will be used to visualize the differences in the flame structure with and without oscillations.

Work Statement For Third Year

Task 1: Continue cold flow investigation of the effects of transverse and three-dimensional acoustic excitation on jets.

Task 2: Further investigate the effects of various modes of acoustic oscillations upon pyrolysis rate using dry ice sublimation as a model of pyrolyzing solid waste.

Task 3: Investigate the effect of transverse mode acoustic excitation on the rate of combustion and evaporation of liquid waste surrogates.

Task 4: Investigate the effect of acoustic excitations on the level of soot, NOx, CO, CO_2 and unburned hydrocarbons in the exhaust of the simulated incinerator while burning solid surrogate wastes.

Task 5: If time permits, use acetone, O_2 and OH PLIF to visualize the flame structure with and without oscillations.

References

1) Patera, A. T. and Mikic, B. B., "Exploiting Hydrodynamic Instabilities: Resonant Heat Transfer Enhancement", Int. J. Heat Mass Transfer, Vol. 29, No. 8, pp. 1127-1138, 1986.

2) Ghaddar, N. K., Magen, M., Mikic, B. B., and Patera, A. T., "Numerical Investigations of Incompressible Flow in Grooved Channels, Part 2: Resonance and Oscillatory Heat-Transfer Enhancement", J. Fluid Mech., Vol. 168, pp. 541-567, 1986.

3) Hodgins, J. W., Hoffman, T. W., and Pei, D. C., "The Effect of Sonic Energy on Mass Transfer in Solid-Gas Contacting Operations", Canadian J. of Chem. Eng., pp. 18-24, June 1957.

4) Deck, J. E., Arpaci, V. S., and Keller, J. O., "Heat Transfer in the Oscillating Turbulent Flow of Pulse Combustor Tail Pipes", Final Report, Sandia Combustion Laboratories, GRI Contract No. 5084-260-1092, July 1989.

5) Hanby, V. I., "Convective Heat Transfer in a Gas-Fired Pulsating Combustor", Trans. ASME J. of Eng. for Power, No. 1, pp. 48-51, January 1969.

6) Arpaci, V. S., Dec, J. E., and Keller, J. O., "Heat Transfer in Pulse Combustor Tailpipes", Proceed. of Int. Symposium on Pulsating Combustion, Sponsored by Sandia National Laboratories and the Gas Research Institute, Monterey, CA, August 1991.

7) Merkli, P. and Thomann, H., "Transition to Turbulence in Oscillating Pipe Flow", J. Fluid Mech., Vol. 68, Part 3, pp. 567-575, 1975.

8) Vermeulen, P. J., Odgers, J., and Ramesh, V., "Acoustic Control of Dilution-Air Mixing in a Gas Turbine Combustor", ASME J. of Eng. for Power, Vol. 104, No. 4, pp. 844-852, October 1982.

9) Lyman, F. A., and Sabnis, J. S., "Combustion of Captive Coal Particles in Pulsating Flow", Proceed. Symposium on Pulse Combustion Tech. for Heating Applications, ANL/EES-TM-87, pp. 95-104, Argonne National Laboratory, Argonne, IL, 1979.

10) Zinn, B. T., et al, "Development of a Coal Burning Pulsating Combustor for Industrial Power", DOE/ER/10068-T2, Pittsburgh Energy Tech. Center, Pittsburgh, PA, 1983.

11) Bai, T., "Combustion of Liquid Fuels in a Rijke Type Pulse Combustor", PhD. Thesis, Georgia Institute of Technology, Atlanta, GA 1992.

12) Stewart, C. R., Lemieux, P. M., and Zinn, B. T., "Application of Pulse Combustion to Solid and Hazardous Waste Incineration", Proceed. of Intl. Symposium on Pulsating Combustion, Sponsored by Sandia National Laboraories and the Gas Research Institute, Monterey, CA 1991.

13) Cantwell, B. J., "Organized Motion in Turbulent Flow," *Ann. Rev. Fluid Mech.*, No. 13, pp. 457-515, 1981.

14) Ho, C. M. and Huerre, P., "Perturbed Free Shear Layers," *Ann. Rev. Fluid Mech.*, No. 16, pp. 365-424, 1984.

15) Zaman, K. B. M. Q. and Hussain, A. K. M. F., "Vortex Pairing in a Circular Jet Under Controlled Excitation, General Jet Response" *J. Fluid Mechanics*, Vol. 101, pp. 449-491, 1980.

16) Zaman, K. B. M. Q. and Hussain, A. K. M. F., "Turbulence Suppression in Free Shear Flows by Controlled Excitation," *J. Fluid Mechanics*, Vol. 103, pp. 133-159, 1981.

17) Ahuja, K. K., Lepicovsky, J., Tam, C. K. W., Morris, P. J., and Burrin, R. H., "Tone-Excited Jet, Theory and Experiments," NASA Contract Report 3538, 1982.

18) Ho, C. M. and Huang, L. S., "Subharmonics and Vortex Merging in Mixing Layers," *J. Fluid Mech.*, No. 119, pp. 443-473, 1982.

19) Parekh, D. E., Reynolds, W. C., and Mungal, M. G., "Bifurcation of Round Air Jets by Dual-Mode Acoustic Excitation," AIAA Paper No. 87-0164, 25th Aerospace Sciences Meeting, 1987, Reno, NV.

20) Juvet, P. J. and Reynolds, W. C., "Entrainment Control in an Acoustically Controlled Shrouded Jet," AIAA Paper No. 89-0969, 2nd Shear Flow Conference, 1989, Tempe, AZ.

21) Ogawa, N., Maki, H., and Kuroda, K., "Studies on Tone-Excited Jet", *Transactions of the Japan Society of Mechanical Engineers, Part B*, Vol. 59, No. 566, pp. 2975-2981, 1993.

22) Matta, L. M., Zhu, C., Jagoda, J. I., and Zinn, B. T., "Gas Phase Mixing Due To Resonant Acoustic Oscillations in a Cavity," AIAA Paper No. 95-0496, 33rd Aerospace Sciences Meeting, 1995, Reno, NV.

23) Lee, M. and Reynolds, W. C., "Bifurcating and Blooming Jets," AFOSR Final Technical Report, Grant No. AF-F49620-84-K-0005, August 1985.

24) Everson, R., Manin, D., Sirovich, L., and Winter, M., "Quantification of Mixing and Mixing Rate from Experimental Observations," AIAA Paper No. 95-0169.

25) Vlasov, E.V. and Ginevskii, A.S. "The Aeroacoustic Interaction Problem (review)," Sov. Phys. Acoust., Vol. 26, pp. 1-7, (1980).

26) Crow, S.C. and Champagne, F.H., "Orderly Structure in Jet Turbulence," Journal of Fluid Mechanics, Vol. 48, pp. 547-592 (1971).

27) Lepicovsky, J., Ahuja, K. K., Brown, W. H., and Morris, P. J., "Acoustic Control of Free Jet Mixing," AIAA-paper No. 85-0569.

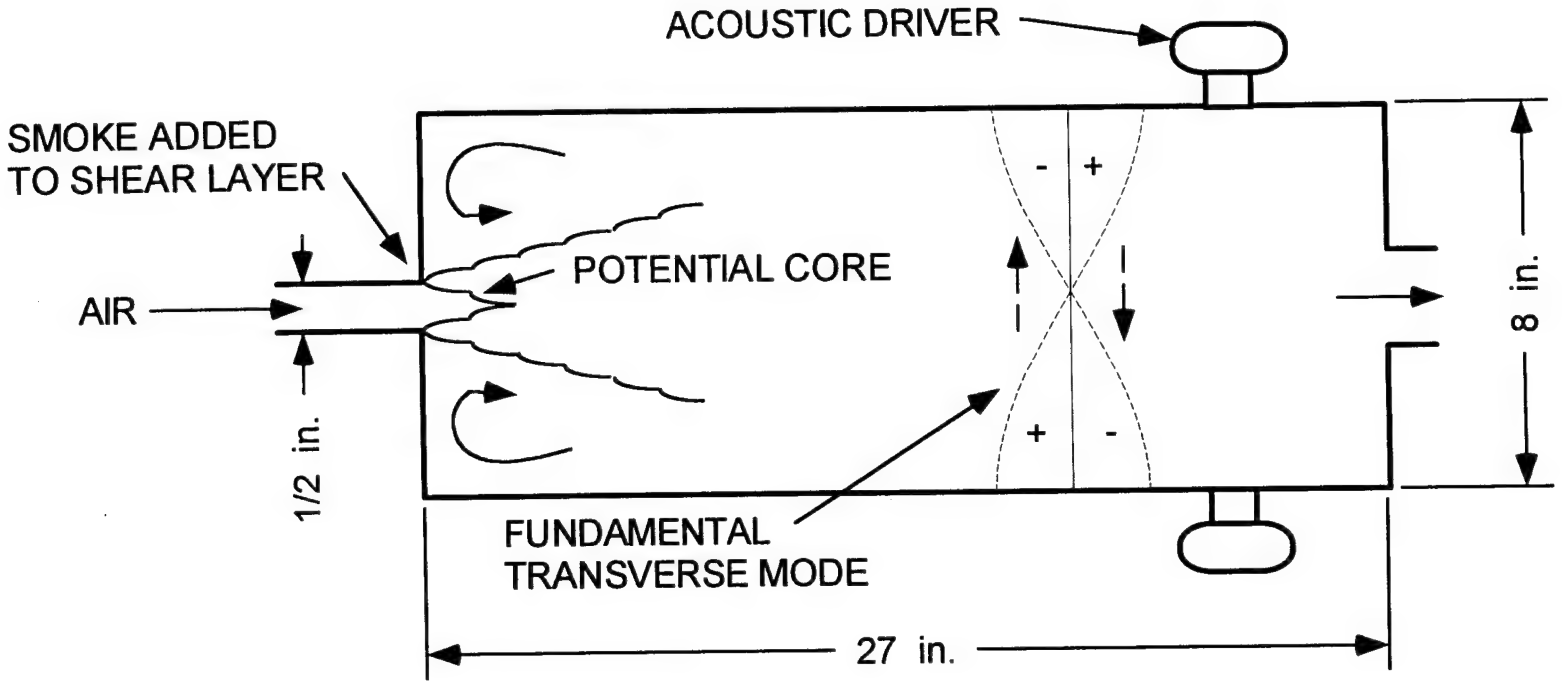

Figure 1. Schematic of Jet Mixing Setup

a) no excitation

b) 855Hz, 150dB excitation

Figure 2. Circular jet with a) no excitation, and b) transverse excitation directed up and down in the picture.

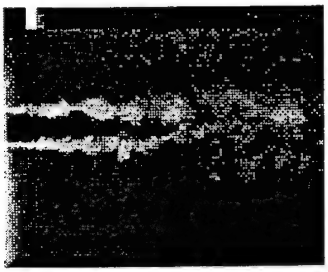

a) no sound

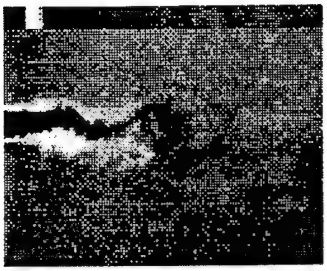

b) 138 dB

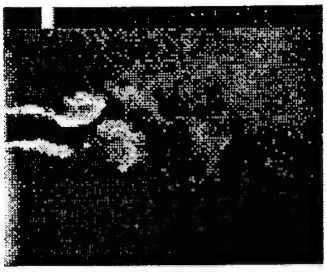

c) 144 dB

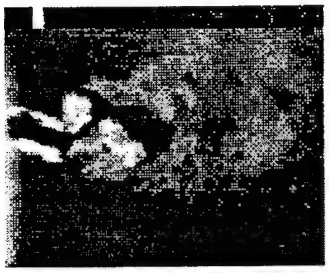

d) 150 dB

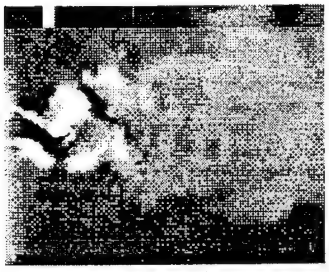

e) 154 dB

Figure 3. Instantaneous images of the excited jet with a velocity of 75ft/s at different amplitudes.

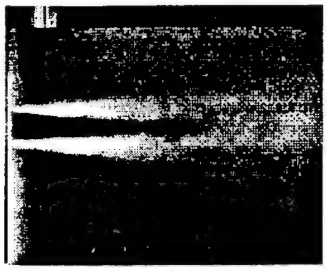

a) no sound

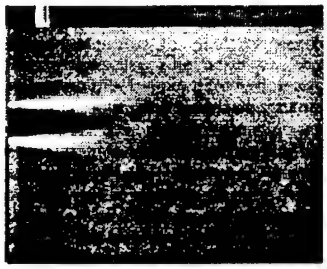

b) 138 dB

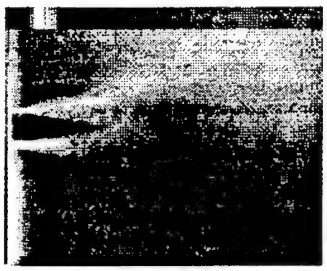

c) 144 dB

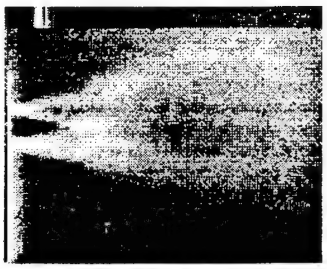

d) 150 dB

e) 154 dB

Figure 4. Time averaged images of the excited jet with a velocity of 75ft/s at different amplitudes.

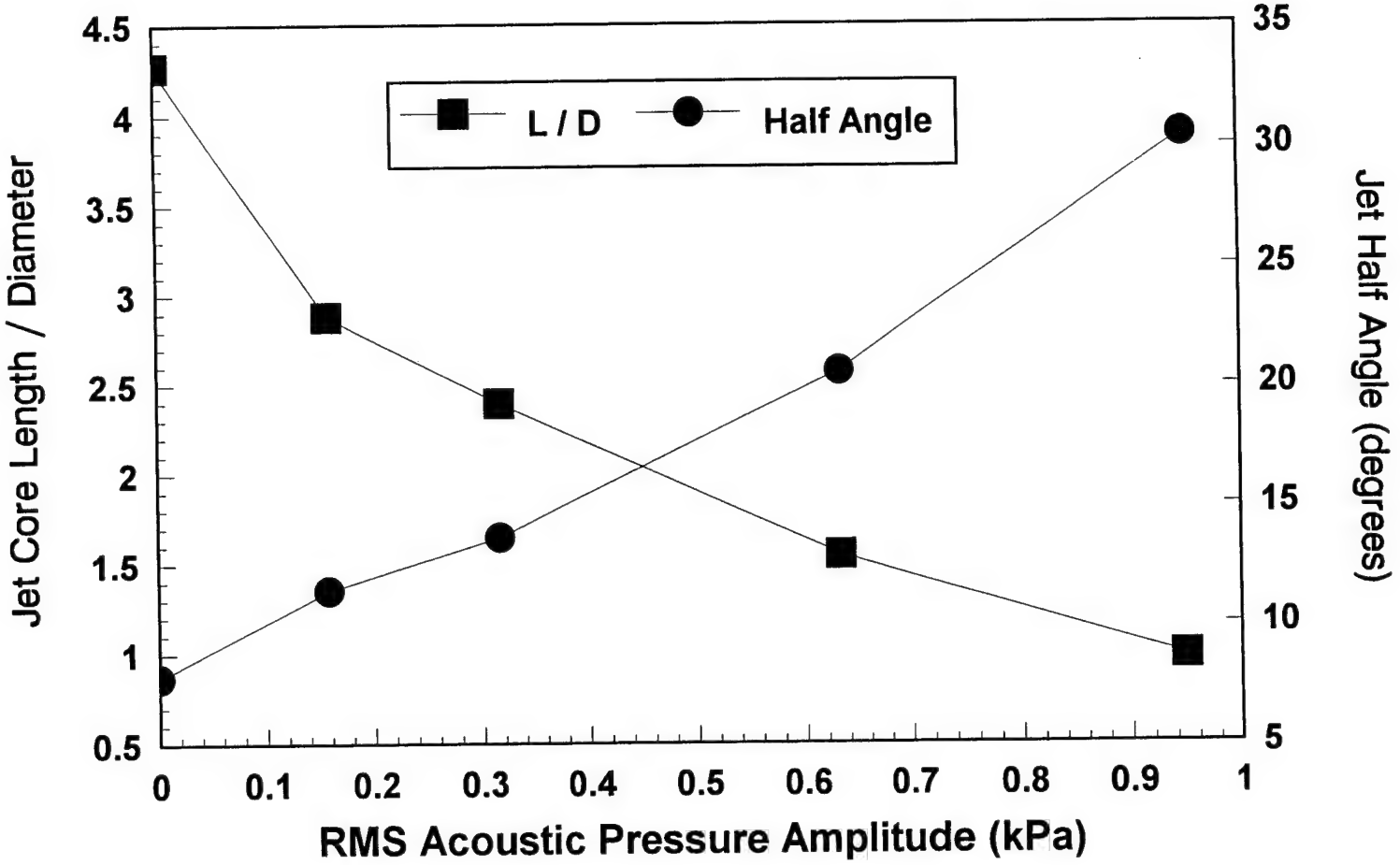

Figure 5. Effect of the oscillation amplitude on the jet..
jet velocity = 31m/s, fundamental transverse mode, f = 855 Hz, St = 0.300

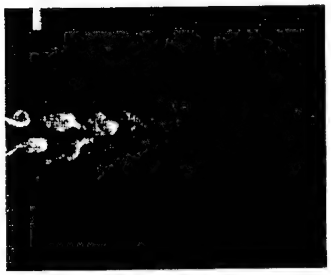

a) 25 ft/s

b) 50 ft/s

c) 75 ft/s

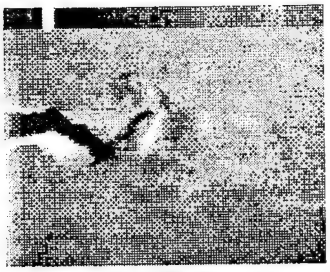

d) 100 ft/s

Figure 6. Instantaneous images of the jet at different speeds excited by a 150dB oscillation.

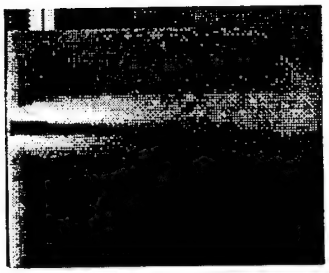

a) 25 ft/s

b) 50 ft/s

c) 75 ft/s

d) 100 ft/s

Figure 7. Time average images of the jet at different speeds excited by a 150dB oscillation.

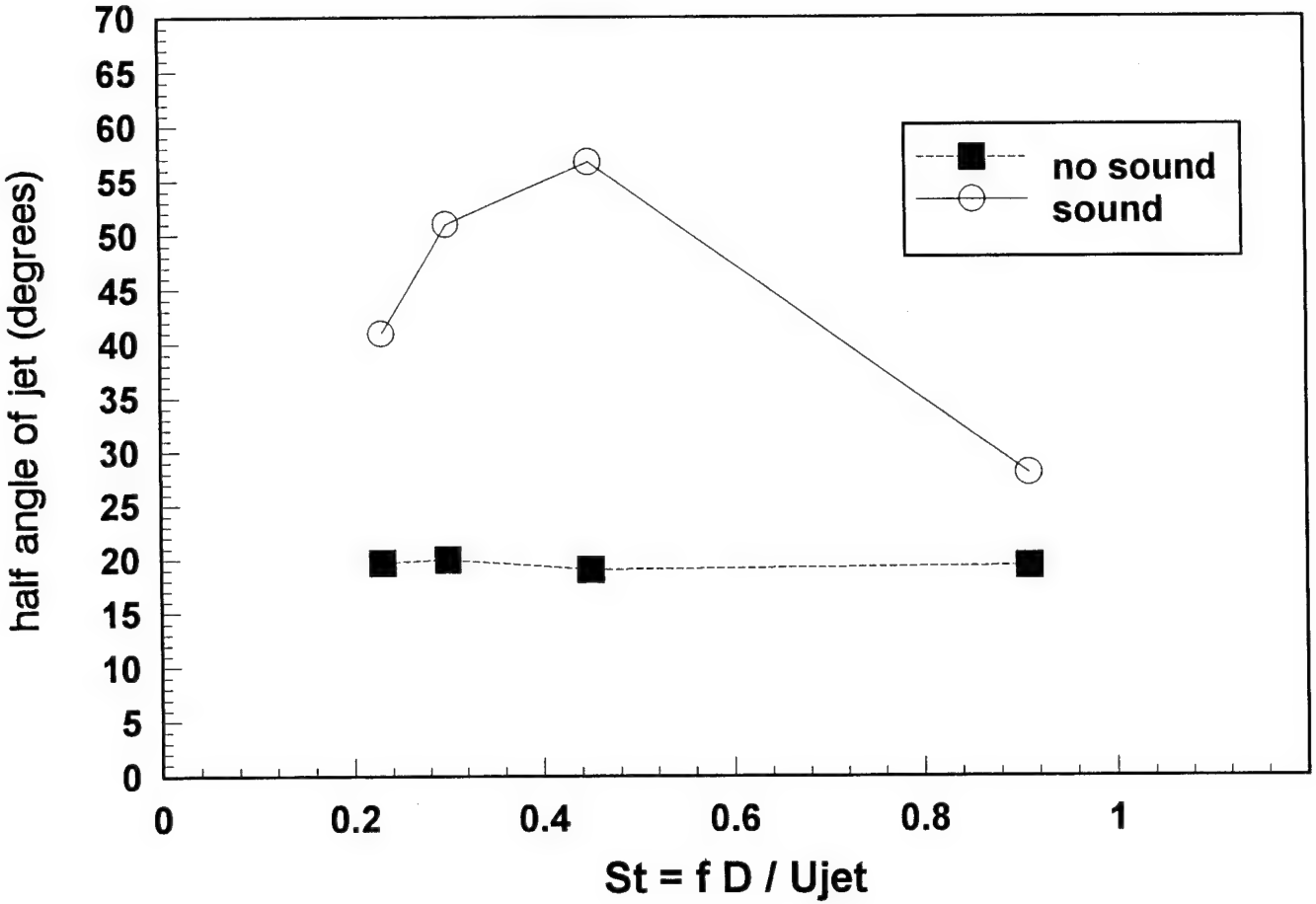

Figure 8. Dependence of the jet core length on Strouhal number.

|p'| = 150dB, fundamental transverse mode, f = 855 Hz

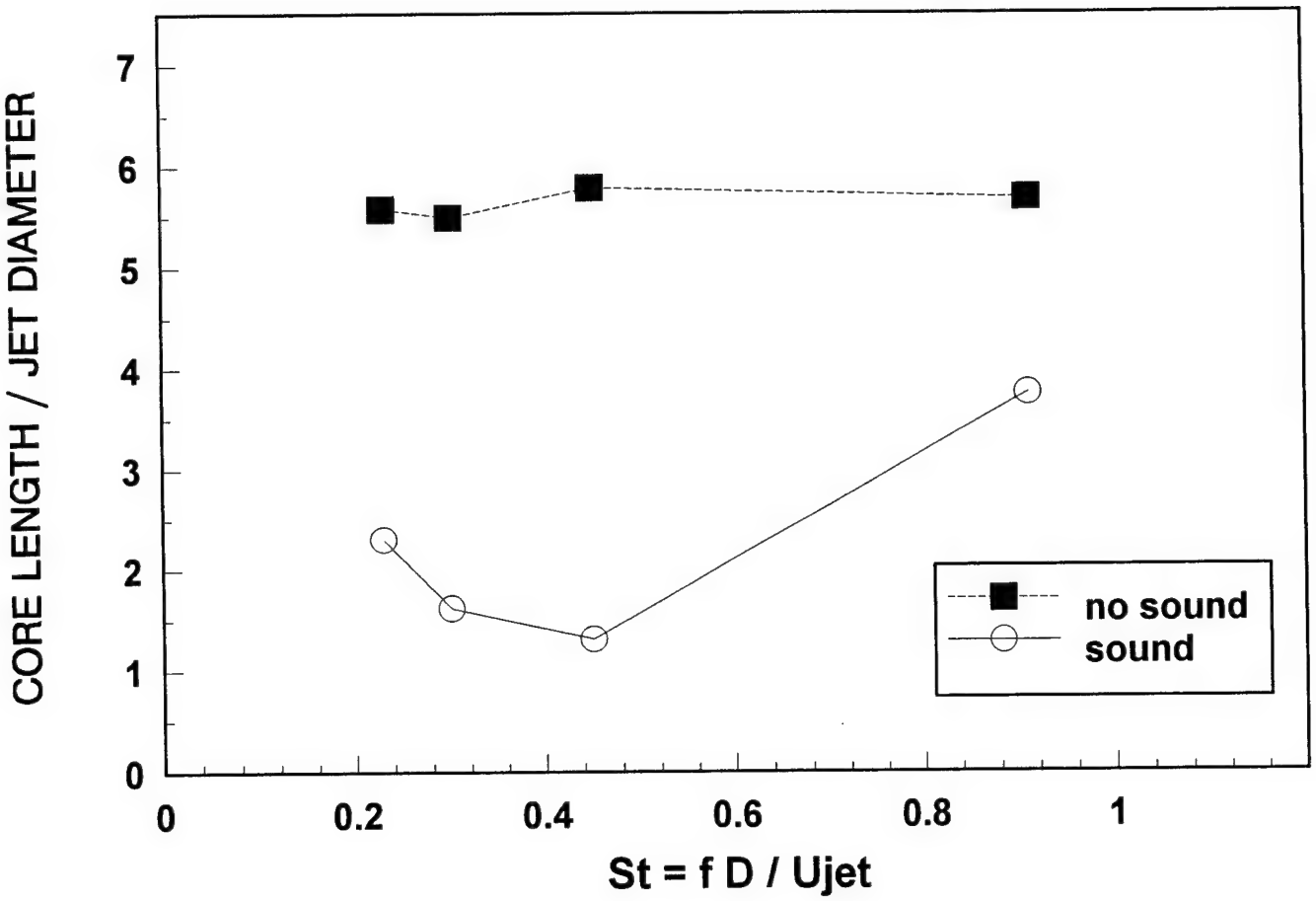

Figure 9. Dependence of the jet core length on Strouhal number.

$|p'|$ = 150dB, fundamental transverse mode, f = 855 Hz

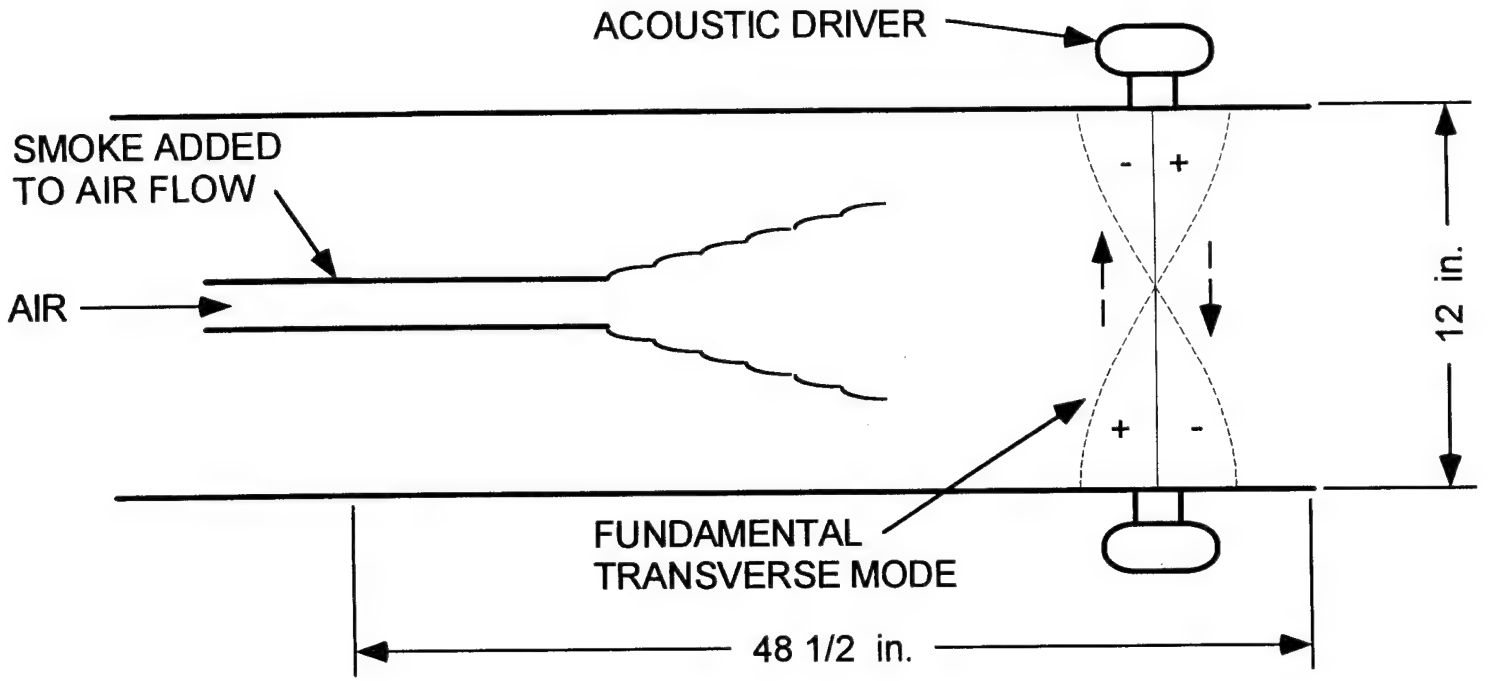

Figure 10. Schematic of Jet Mixing Facility

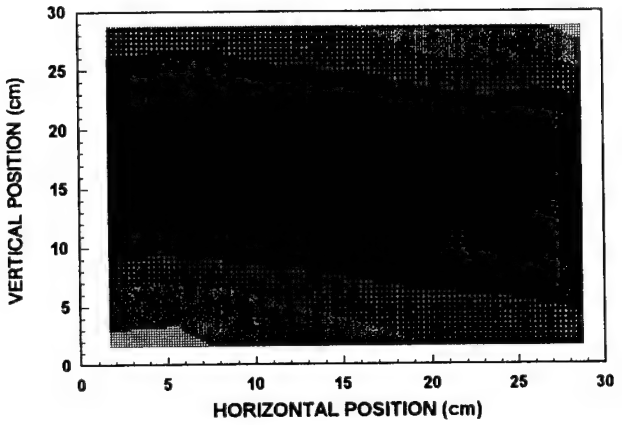

a) 20.3 cm from upstream end

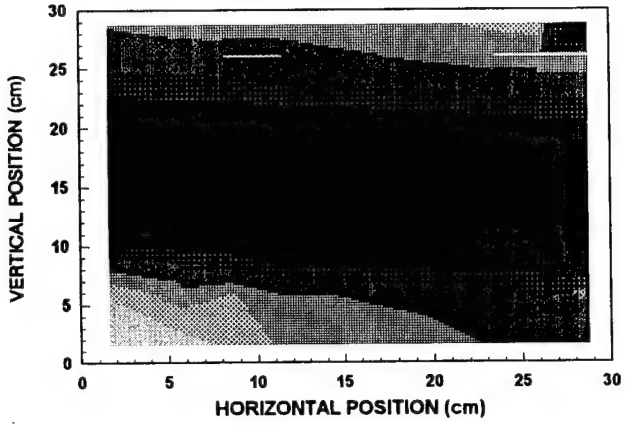

b) 35.6 cm from upstream end

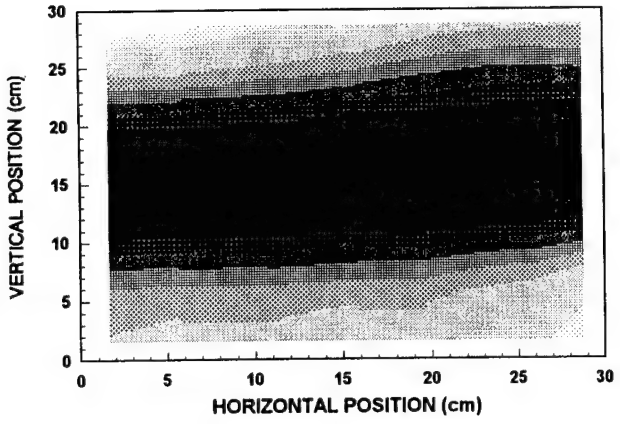

c) 50.8 cm from upstream end

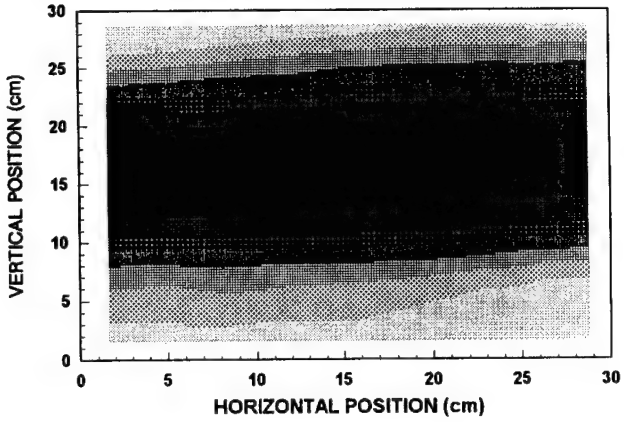

d) 60.0 cm from upstream end

Figure 11. Pressure distributions at four axial locations.

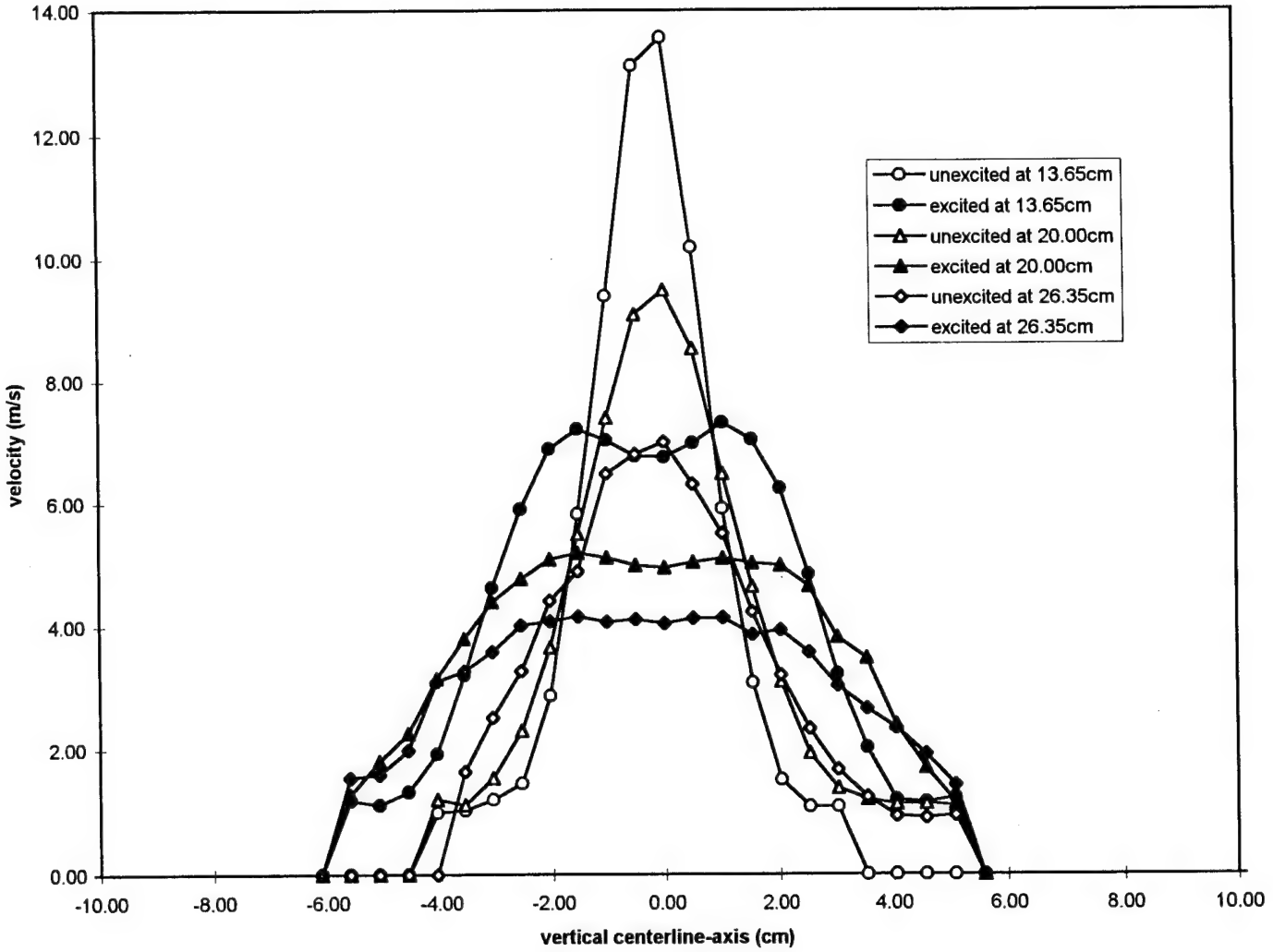

Figure 12. Velocity profiles of a jet with an exit velocity of 22.13m/s in the direction of a 132dB oscillation.

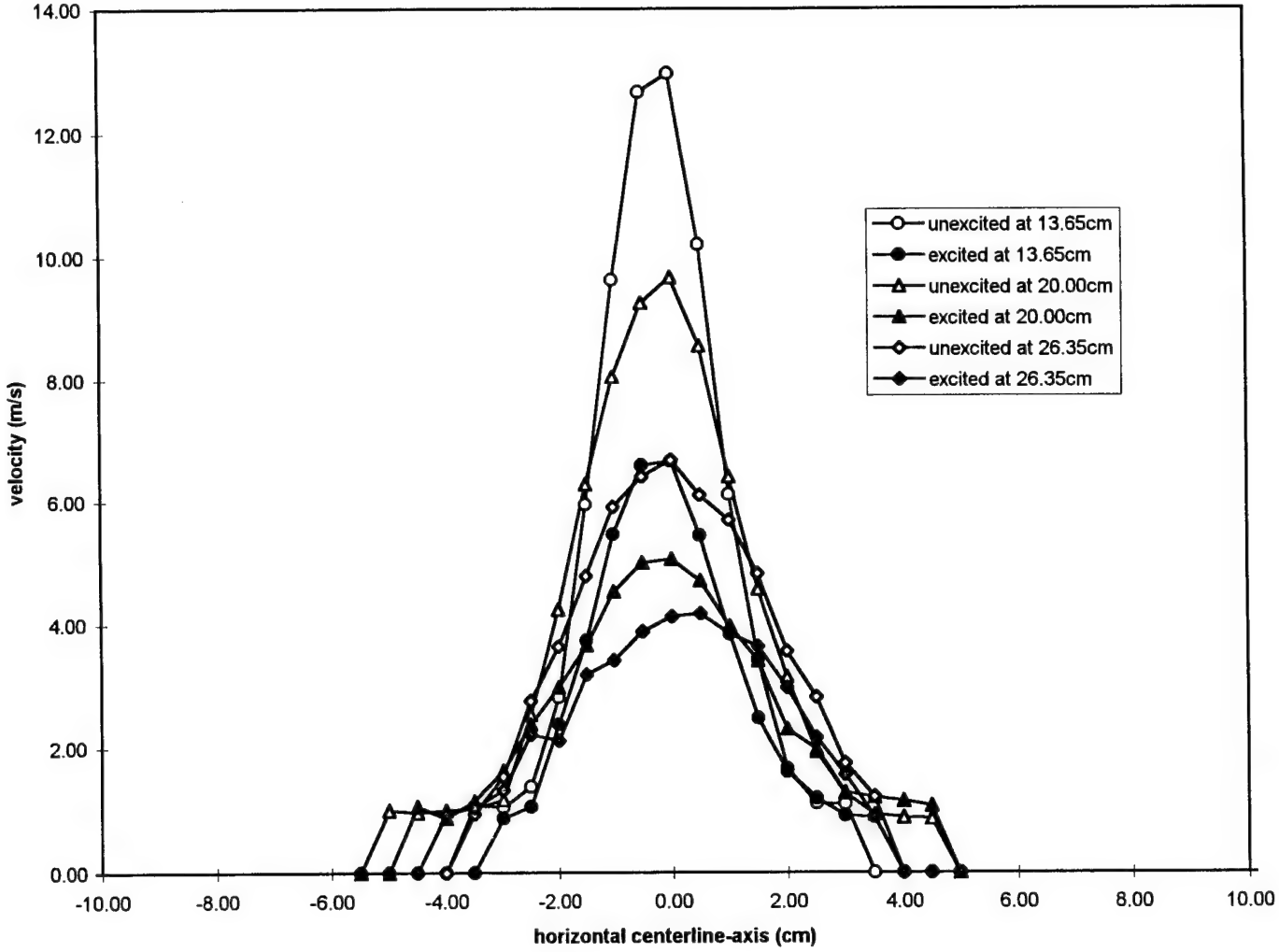

Figure 13. Velocity profiles of a jet with an exit velocity of 22.13m/s perpendicular to a 132dB oscillation.

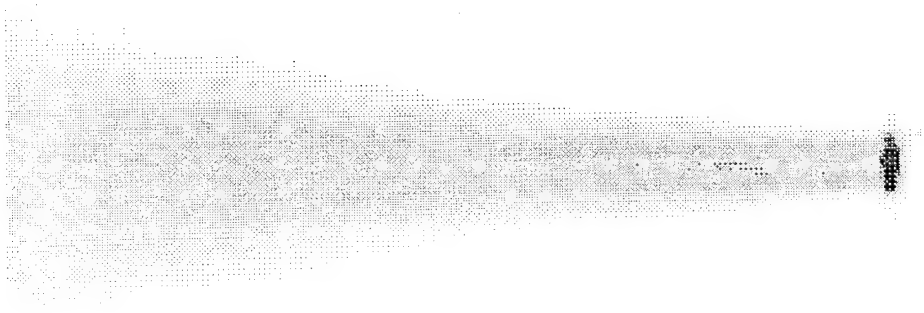

a) No acoustic oscillation present

b) 132dB, 855Hz oscillation present

Figure 14. Phase-locked, averaged images of a jet excited by transverse acoustic oscillations.

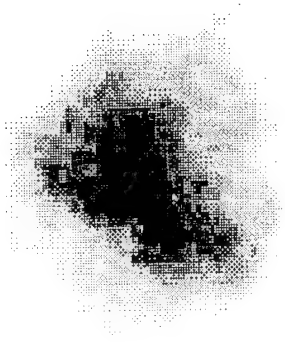

a) No acoustic oscillation present

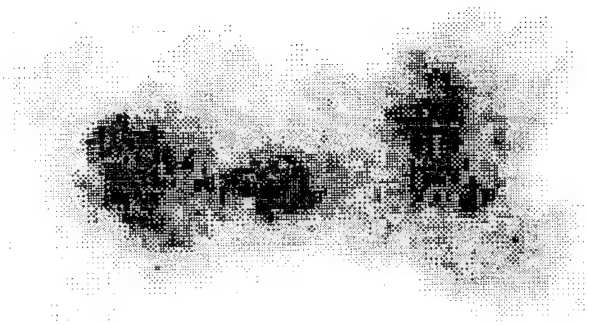

b) 134dB, 855Hz oscillation present

Figure 15. Instantaneous cross-sectional images of a jet excited by transverse acoustic oscillations.

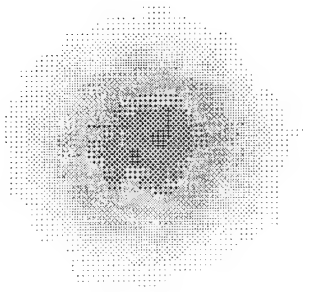

a) No acoustic oscillation present

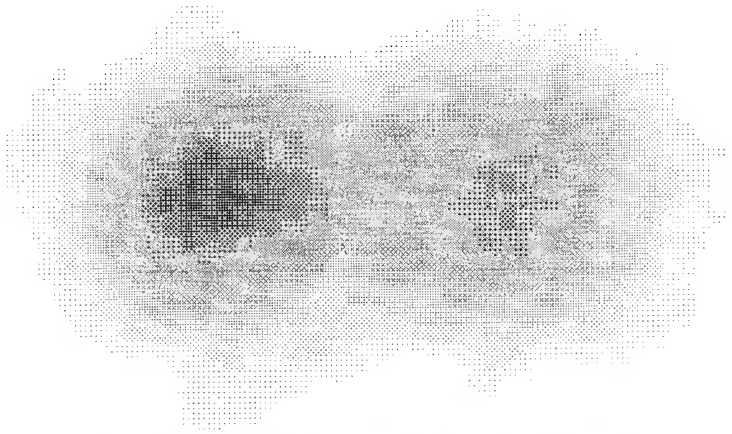

b) 134dB, 855Hz oscillation present

Figure 16. Phase locked, averaged cross-sectional images of a jet excited by transverse acoustic oscillations.

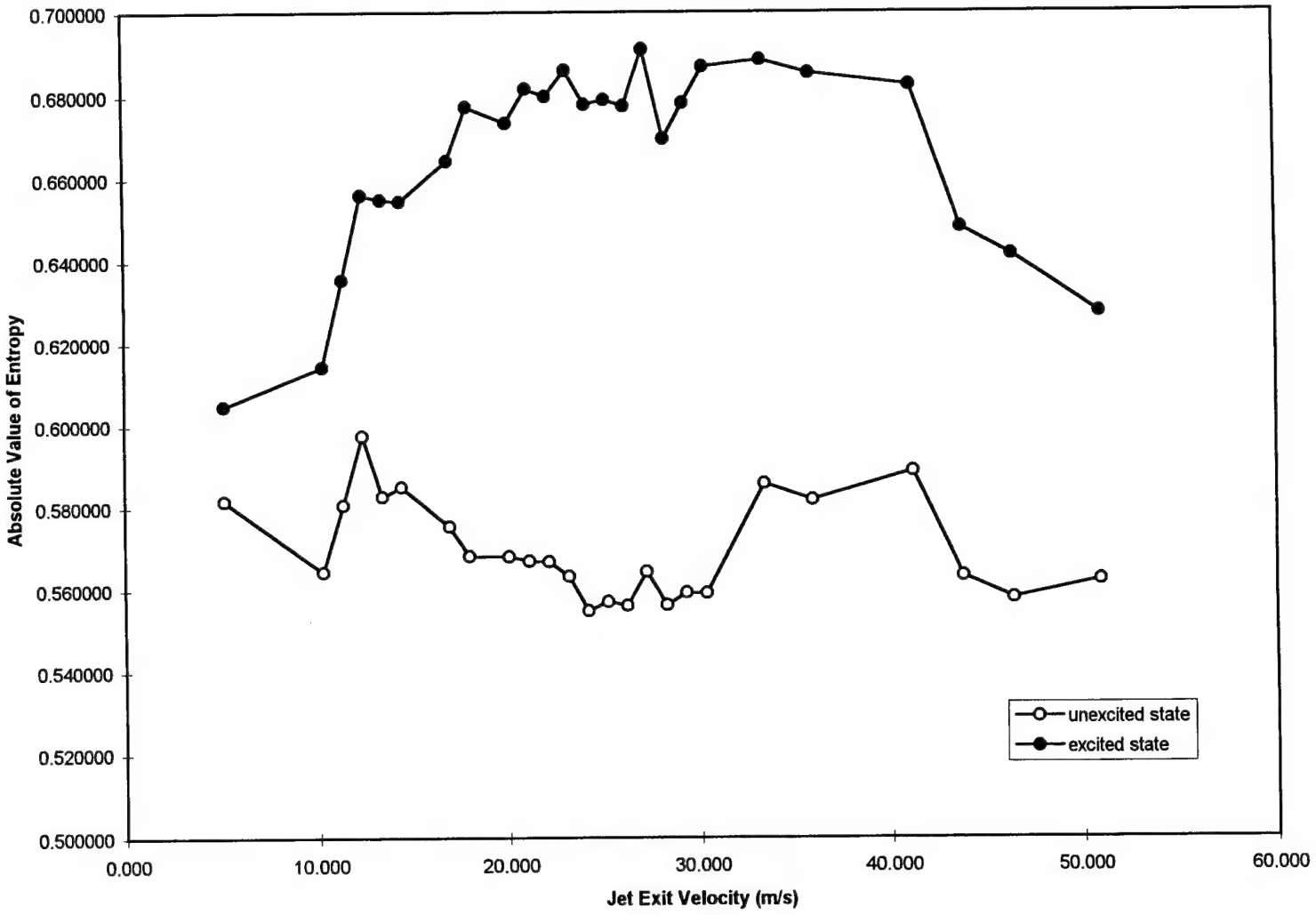

Figure 17. Mixing entropy without and with 134 dB oscillations measured 13.65cm downstream of the jet exit.

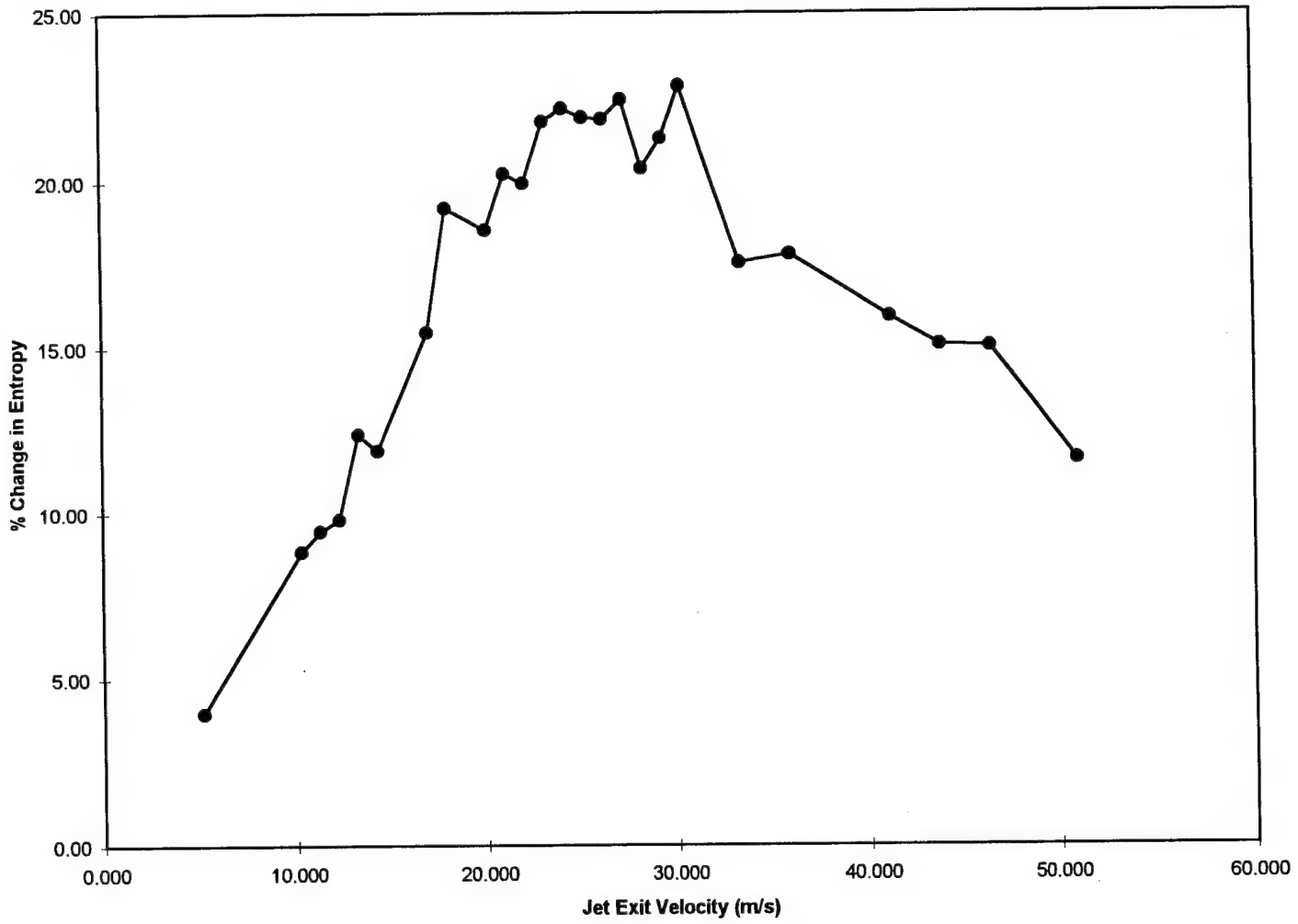

Figure 18. Increase in the mixing entropy value due to the presence of 134dB oscillations.

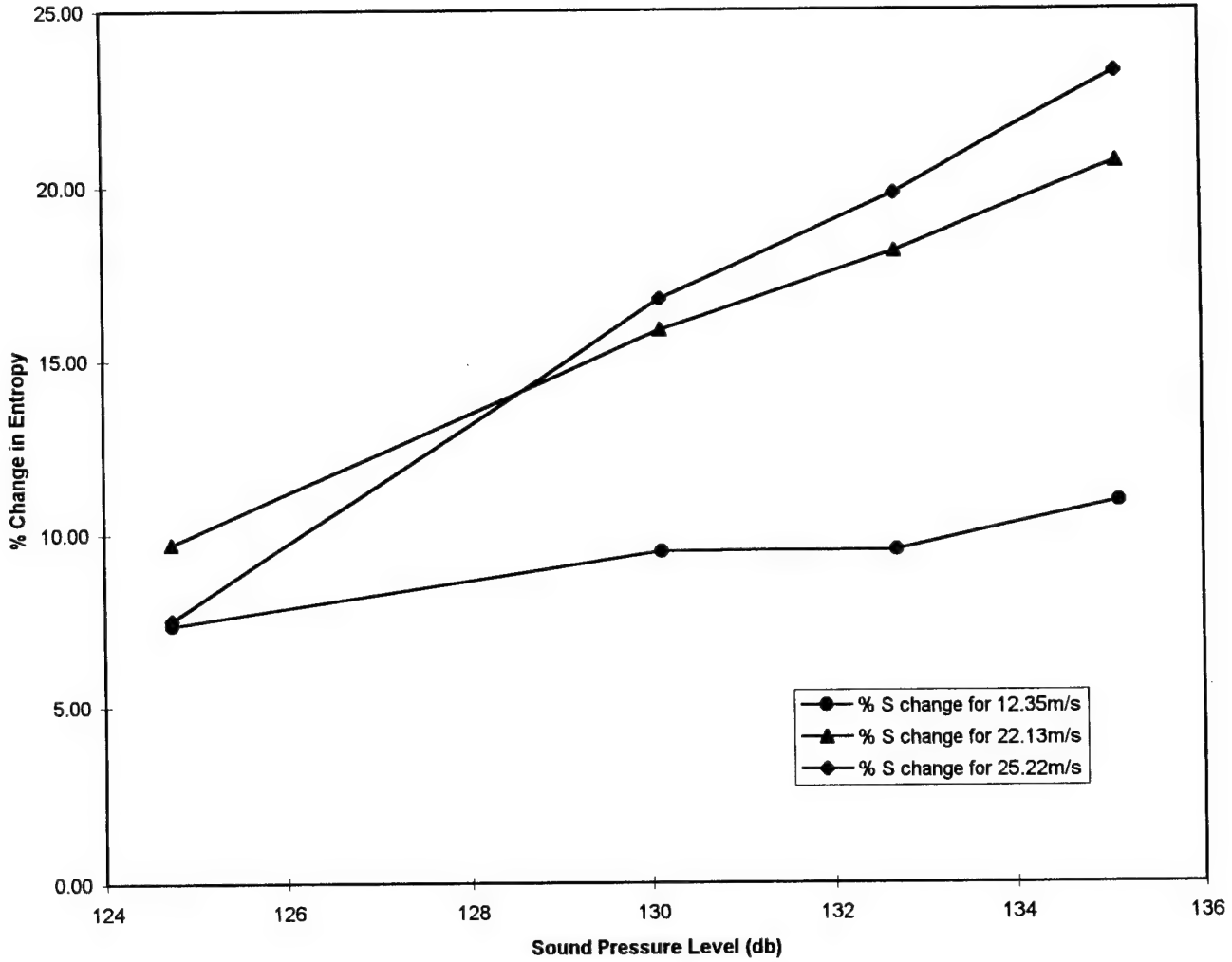

Figure 19. Effect of the oscillation amplitude on the change in mixing entropy.

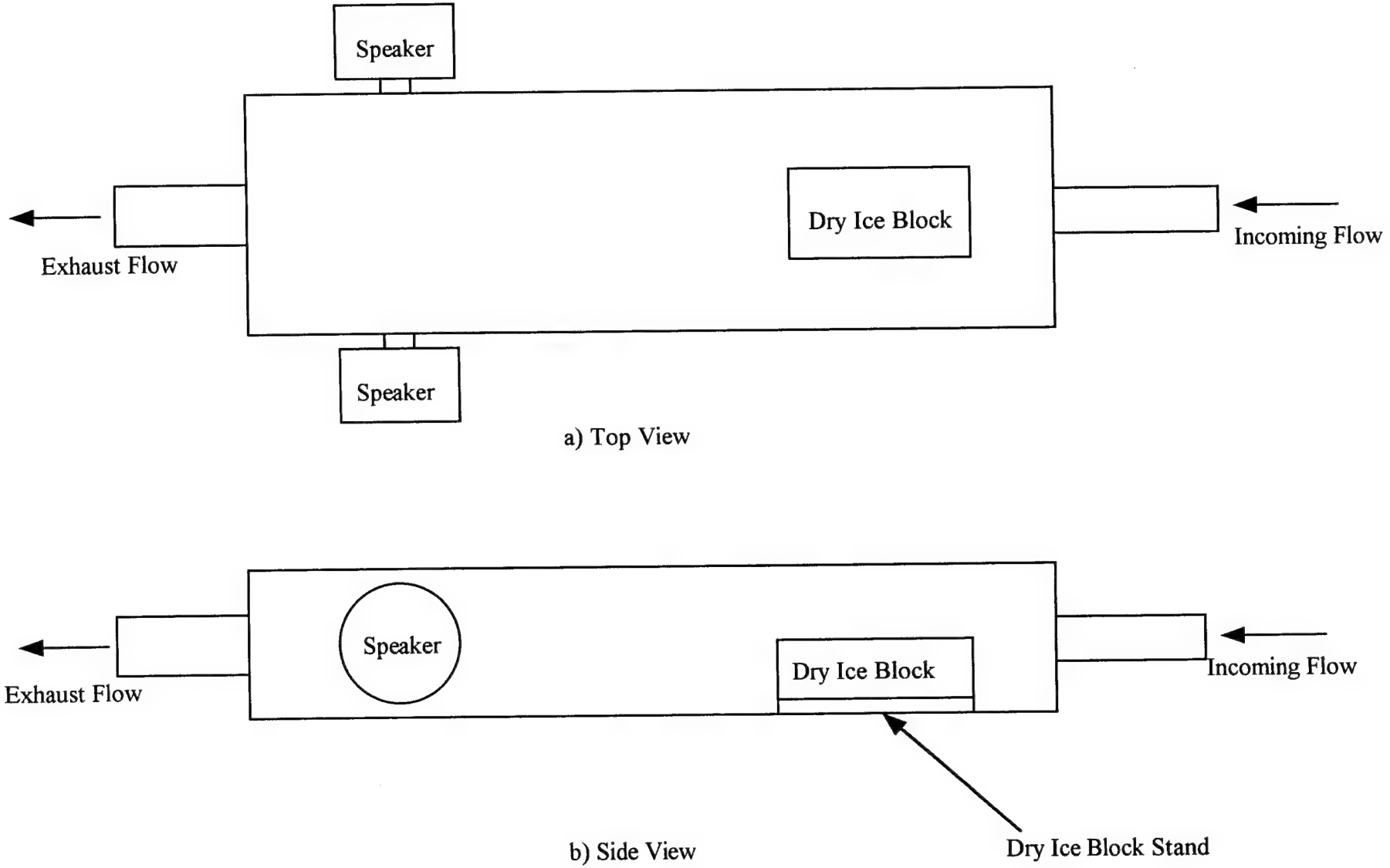

Figure 20: Schematic of the dry ice sublimation facility.

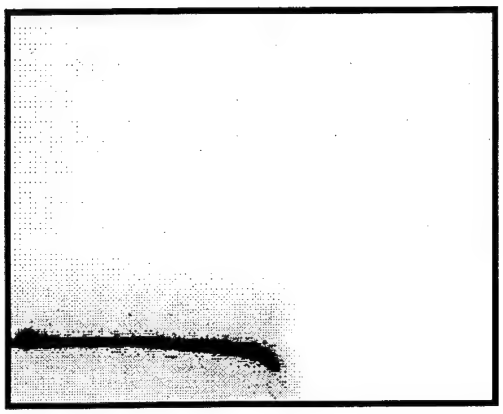

a) no oscillation, no mean flow

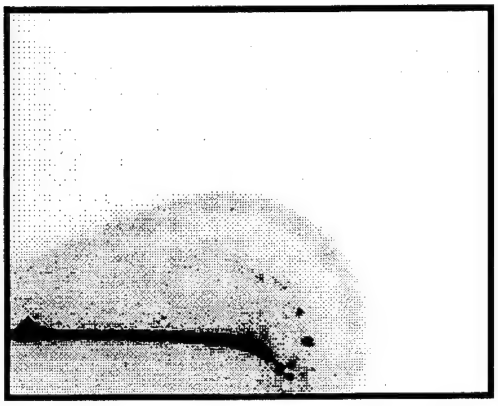

b) 150dB oscillation, no mean flow

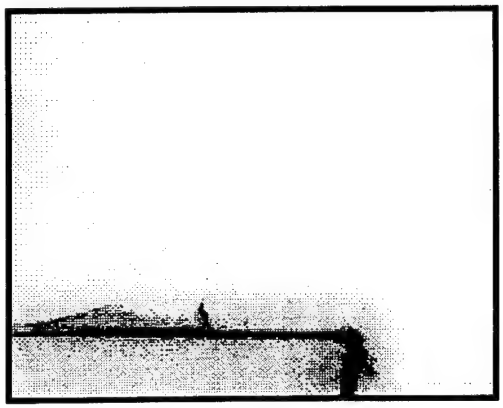

c) no oscillation, 0.5m/s mean flow

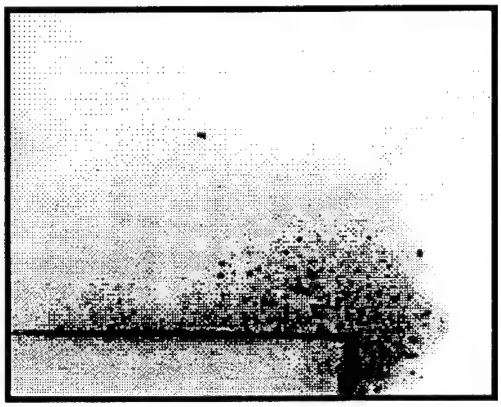

d) 150dB oscillation, 0.5m/s mean flow

Figure 21. Images of the fhe fog layer at the downstream corner of the dry ice block under various conditions.

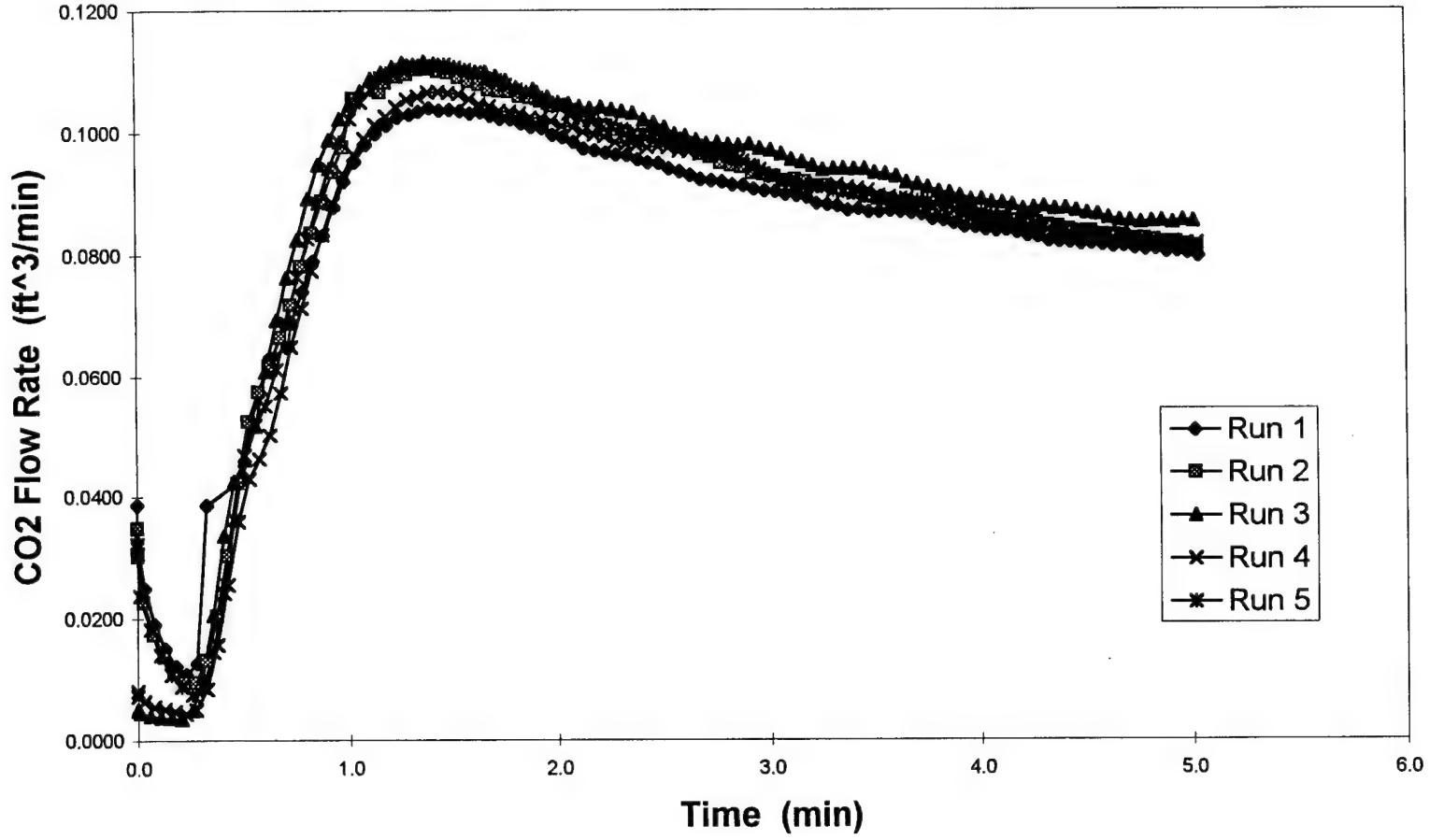

Figure 22. Carbon dioxide exhaust flow rate with a 1 m/s air inlet flow and no acoustic oscillations.

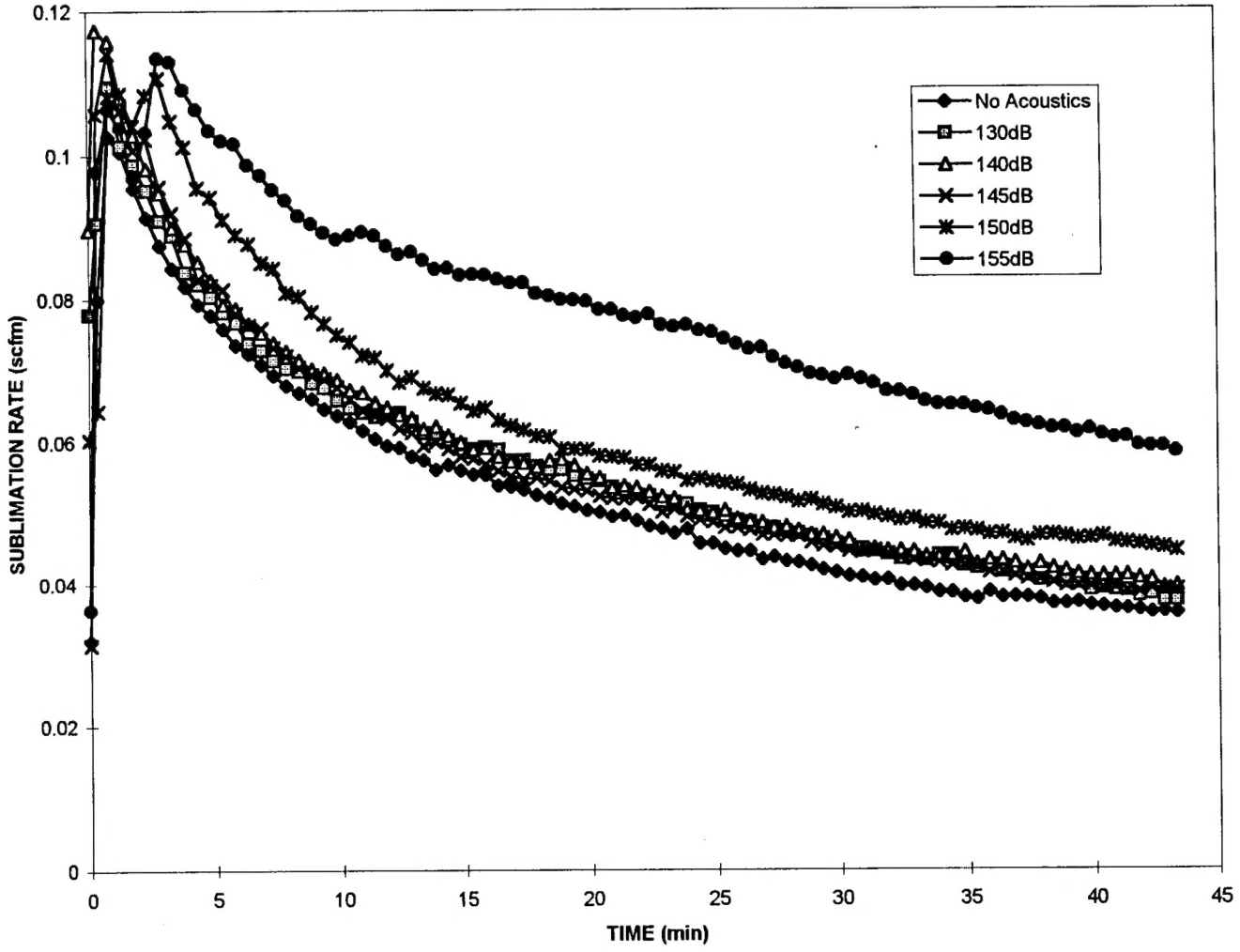

Figure 23. Carbon Dioxide exhaust flow rate with a 1m/s air inlet velocity at various amplitudes of acoustic oscillation.

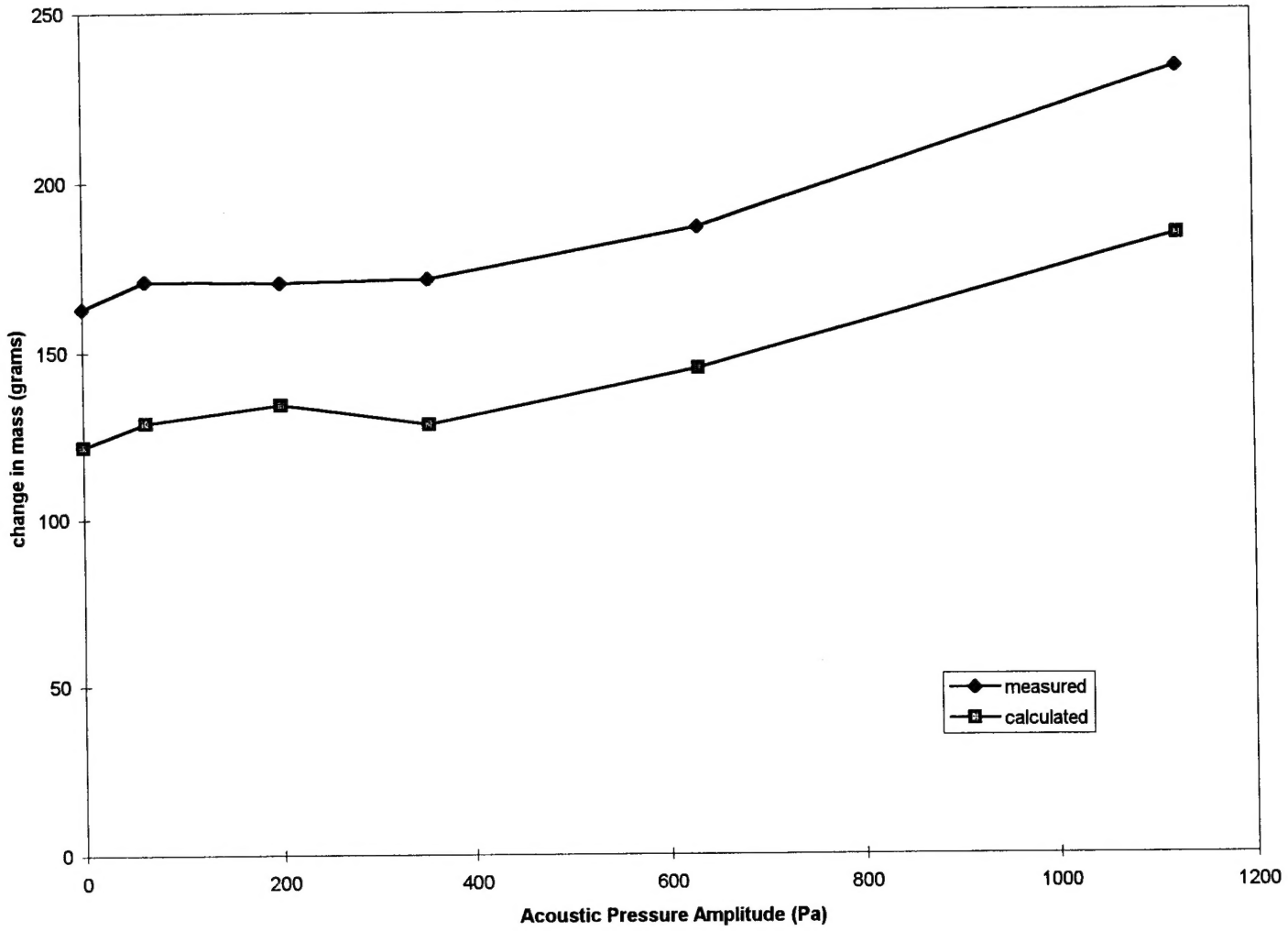

Figure 24. Comparison of the measured total mass sublimation to the amount calculated from exhaust sampling.

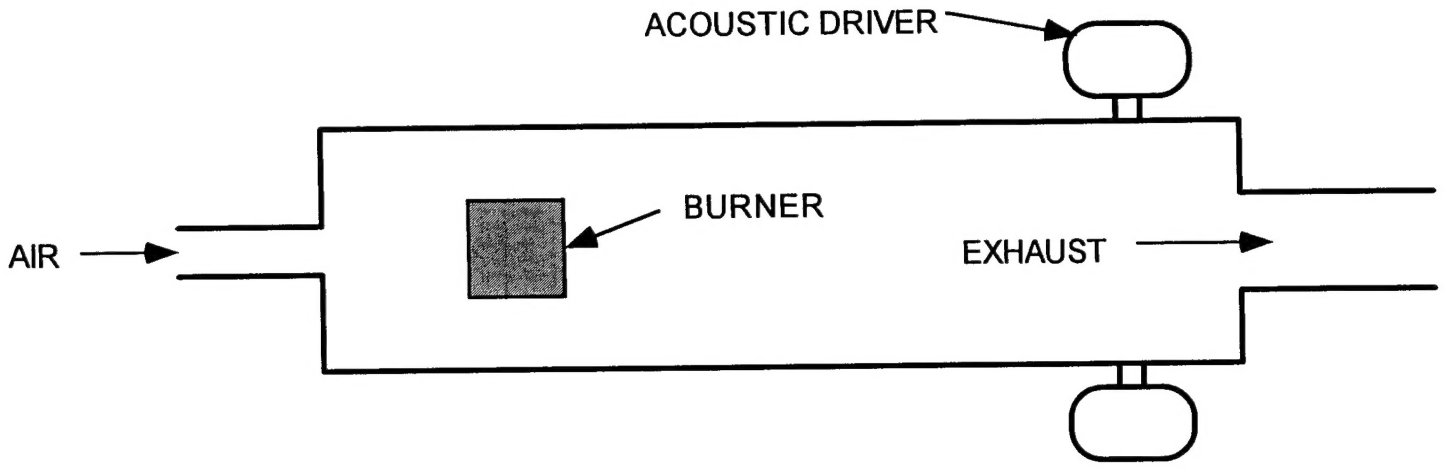

a) Top View

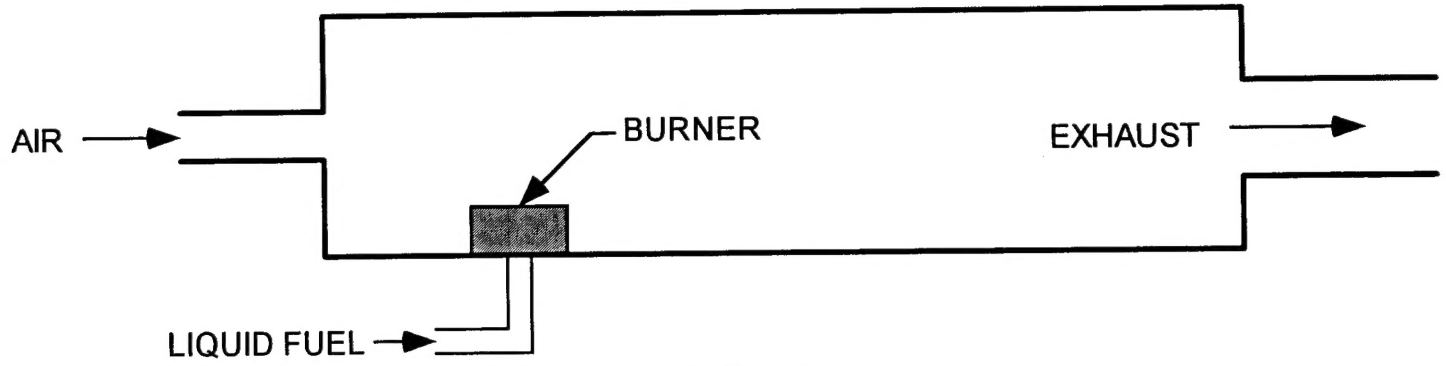

b) Side View

Figure 25. Schematic of the pulsed incineration facility.

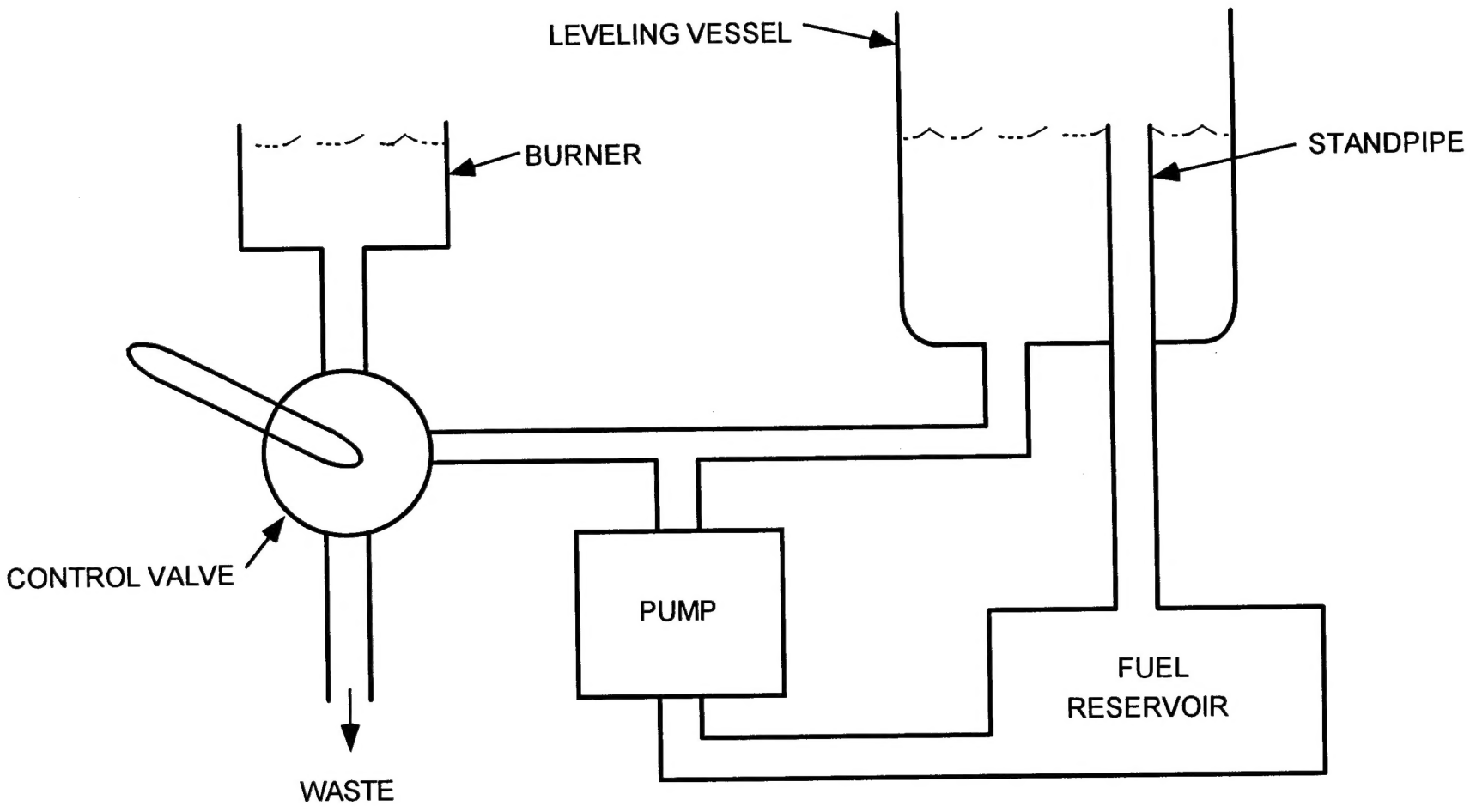

Figure 26. Schematic of the liquid fuel supply system.